Answers to referees:
Effects of Black Carbon Mitigation on Arctic Climate

We thank the referees for their interest and their time invested in reviewing our manuscript. Thank you also for the constructive comments you made. Please find our answers to your comments in the sections below.

Referee 1:

1. Section 3.1 is a bit confusing – some clarifications in the text will do much to improve this section

   We re-wrote Section 3.1 to make it easier to understand for the reader.

2. The discussions of how BC and OC influence clouds are solely focused on indirect aerosol effects. Firstly, a short discussion of how BC and OC particles are thought to act as cloud condensation nuclei would improve these discussions. My impression is that while BC particles can act as CCN when duly coated, it is not thought to be as efficient a CCN as OC, which is hygroscopic to begin with. Even so, certain models have been shown to have very strong indirect aerosol effects from BC. A comment of the validity of such model results could be added here. Secondly, numerous studies have shown that BC potentially cause strong rapid adjustments in clouds, but perhaps more importantly due to its influence on the vertical temperature profile and water vapor levels (semidirect effects) than due to the indirect aerosol effects. This should also be discussed in the paper.

   We have included a more detailed description of how SU, BC, and OC affect cloud activation. We have also added discussion on semi-direct effects of BC through changes in vertical temperature profiles, water vapour, and cloud dynamics.

3. P1 L19: This important information is difficult to assess in absolute numbers, as we do not have any reference points. Is it possible to rather give the % change in premature deaths?

   We added the change in % to the abstract and the main text. Note also that there was a typo in the abstract: the amount is 329000, not 339000. We corrected this as well.

4. P2 L7: Several studies have pointed to the fact that the direct radiative heating effect of BC is in fact offset by rapid adjustments in clouds. Perhaps consider adding some of these references here, and also mention that semidirect effects may be just as or more important than indirect effects in this regard.

As mentioned above, we have added discussion on the importance of semi-direct effects of BC aerosol together with appropriate references.

5. P2 L14: Please add references after "gas industry".

   We added references as requested.

6. P6 L21: Please add "2010 – 2030" before "emission reduction", to be entirely clear that the reader is to look at changes along the x axis in Fig. 2 at this point. The statement that OC and BC emissions are mostly unchanged is also not obvious from Fig. 2 – a change of about 1 Tg/yr in BC from 7.2 or so in 2010 to 6.2 or so in 2030 is after all 10-15%, which is definitely a change. SU seems to change by about 100 to about 80 over the same period, which is around 20%, so in other words relatively comparable to the BC change? I realize that I may be misunderstanding here, but if so that just underlines the need for some clarifying comments in the text.

   You are absolutely right about the size of the changes in BC and OC. We entirely re-wrote Section 3.1 to make it easier to understand. This includes re-structuring the text and adding percentages of the changes in emission strengths for BC, OC and SU.

7. P6 L22: Please specify in the text that no information on CO2 can be found in Fig. 2.

   We entirely removed the discussion about CO_2 from this Section to avoid confusion.

8. P7 L1: See two comments up – this information is excellent, but it would help the reader to provide it further up in the text. Please also give percentage changes for BC and OC emission reductions, for instance for CLE and GLOB, respectively?

   As stated under comment 6, we rewrote Section 3.1 and included the requested numbers.

9. P12 L31: Somewhere in this section, it would be good to see a discussion of how well SU, BC and OC function as CCN in the ECHAM model.

   In the cloud activation routine, SU and OC are treated as fully dissolved compounds with hygroscopicity value k of 0.57 and 0.21, respectively. BC is assumed to be completely insoluble and contributes to cloud droplet activation by facilitating condensation of sulfuric acid to the particle phase and affecting the size of activating cloud droplets. We added this description to the Methods section (Section 2.2).

10. P14 L8: "the warming effect of SU reductions" → "the direct warming effects of SU reductions", or "the SU warming effects due to aerosol-radiation interactions"

    Thank you for the input, we changed the text accordingly.

11. P14 L16: Please point the reader to where in the vertical profiles we see signs of that upward shift. Also, are we sure that the temperature profile doesn't shift too? If so, there's not necessarily more ice clouds, just liquid clouds higher up. Please comment on this. Here, it would also be nice to mention that, as seen in Fig. 6a moving from CLE to AC – the most local mitigations, which cause strong changes in lower-atmosphere but little changes in

upper-atmosphere BC concentrations (Fig. 4), has a very little influence on the direct forcing, presumably due to the low aerosol absorption efficiency at low altitudes.

We added two figures to the supplementary material, Figures S5 and S6. Here the changes in water and ice clouds are visualised separately. The shift in cloud height we were referring to can be seen from the decrease in water cloud occurrence time (Fig. S5, panels c, g, and k) in the lower part of the atmosphere, a similar decrease in ice cloud occurrence time in the lower part of the atmosphere (Fig. S6, panels c, g, and k), and an increase in ice cloud occurrence time in the upper part of the atmosphere. However, these effects are very small and, as referee #3 remarked statistically not significant. We therefore removed this statement.
Concerning the statement about Arctic direct forcing due to BC emission changes, assuming here that the referee is referring to Figure 7a, this is a valid point. We pointed this out in the manuscript and added some references.

12. P14 L29: This is a good point, concerning the increased aerosol absorption efficiency of BC with height. The literature on this is extensive, so a reference here would be good!

    We added references to previous literature that have pointed out that the absorption efficiency of BC varies with height.

13. P14 L30: "the BC mitigation scenarios" is a term not used before – is this equivalent to "SLCF scenarios". If so, make this clear to avoid confusing the reader.

    Thank you for pointing this out – we corrected the text accordingly.

14. P14 L30: "Compared to the sRFA values of the BC mitigation scenarios, the sRFA that is caused by the reductions in SU emissions in the CLE scenario is much smaller in magnitude" Please point the reader to where this small(er) reduction in sRFa can be seen – from Fig. 6a, the sRFa increases from 2010 to 2030, and is reduced in 2050. Which, if any, of these are you referring to?

    We added some clarifications to the text and added the corresponding values.

15. P15 L1: "systematically" is perhaps a bit strong – it does not seem that sRFa for CLE and AC follow the BC emissions in the same way as the other scenarios

    Agreed. We changed the wording from "systematically" to "fairly well".

16. P15 L6: Here, on the other hand, I don't agree that there is no visible systematic response in sRFtot to BC/OC reductions: The further away from the Arctic emissions are reduced, the weaker this warming effect in 2030. If I understand correctly, the direct aerosol effect will be included in this tot effect, and as you saw in panel a, this component is more strongly negative moving from AC towards GLOB. Thus, any positive radiative forcing effect is offset the most in GLOB, which causes the weakest positive sRFtot values here.

    We agree entirely with the referee about the sRF_A values being most negative for the GLOB scenario and hence the total indirect contribution here must also be strongest – we will

include this statement in the main text. However, looking at the sRF_{TOT} values (in some sense a short-wave ERF), the five curves are not ordered according to the amount of emitted BC. For instance, the AC curve (blue) is above the CLE curve (black), which would make sense, because AC emits less BC than CLE, but AC is also above AC_ACT (purple), which emits even less BC. Altogether, the differences in sRF_{TOT} between the different scenarios for the same year are not statistically significant. We added this information to the manuscript.

17. P16 L1: "Here the effect of both SU reduction in the CLE scenario and BC and OC reduction in the SLCF scenarios are clearly visible." Could it possibly be also that the small (in relative terms, but perhaps noticeable in absolute terms) reduction in SU between the CLE and the other scenarios is also contributing do this change in CDNC?

    This is of course possible, but looking at the vertical SU profiles, we cannot really verify this assumption. We therefore decided to remain with the conclusion that CDNC changes are mainly caused by BC and OC concentration changes.

18. P16 L12: While the CDNC explanation for the increase in sRFtot is plausible, BC have also been shown to have a strong influence on clouds (rapid adjustments / semidirect effects) via the influence on atmospheric heating. Although this element is not included in the analyses, I think the authors should discuss how it could also contribute to explain the findings.

    We added a statement concerning the semi-direct effects to the manuscript.

19. P16 L13: By "cloud time" in this section – do you mean "cloud lifetime"?

    "Cloud time" here is the accumulated time that a grid box in the model is actually in cloud. Averaging this quantity over a larger region gives a measure of the cloudiness in that region. We explained this better in the manuscript.

20. P16 L28: Here it would be good to mention that this supports earlier findings of BC climate effects – that rapid adjustments in clouds tend to balance out the direct effect.

    We added a statement and references as requested.

21. P18 L1: here you could add ", which cause lower-level changes in BC, " or something similar behind "the Arctic Council member states" Figure 5: Just a simple edit: could you perhaps change the unit of the cloud cover to %? I believe the units on the x axis would be the same, so that you could just change "x10-2" to "(%)".

    Thank you for the suggestion, we added this to the text. We also changed the units in the figure to % as requested.

Referee #2:

1. The manuscript tends to be over-inclusive. Some sections are definitely out of context here, especially Section 3.6 is completely out of topic, as also indicated by the absence of figures in the main text. I suggest removing the above-mentioned section because it does not comply with climatic effects. Something similar might be said for Sections 3.1 and 3.4.1. Global emissions and resulting forcing are definitely of interest, but it is hard to understand what is the goal of such two chapters.

   This article is the outcome of a collaboration of climate lawyers, environmentalists, and climate modellers. Therefore, the manuscript has been written in an attempt to trace the possible climate impact of a political instrument (here the Arctic Council) accounting for all the necessary and resulting changes. This includes the mitigation measures that can/should be implemented, the resulting changes in anthropogenic emission strengths, and finally the expected changes in the atmosphere. The latter includes not only climatic effects but also other effects like, for instance, effects on human health (often labelled as co-benefits). This may not seem very relevant to a climate scientist, but for scientists of other fields and for decision makers this is an important aspect to take into account. Just as an example, constructing an emission scenario that only removes BC is not very realistic, because BC and OC are emitted from the same sources and cannot be separated in reality.
   The reason we discuss the global emissions is to show how much emissions can be reduced vs how much this affects the Arctic. At the same time, health effects are much more local and to be able to discuss these effects a discussion of the emissions is necessary.
   The global radiative forcing is mainly discussed to show the effects of BC and OC vs SU more clearly, because there is so much uncertainty when looking at the Arctic region alone.

2. My major concern is, however, the superficial description of the aerosol-physics module (Section 2.2). As a consequence, it becomes almost impossible to judge the reliability of simulations shown in Figure 3, 7 and 9. This is unfortunately amplified by a consistent lack of references along the entire manuscript. Each statement on aerosol-cloud properties or model performances must be explained with citations or results (see in specific comments below). Interestingly, the conclusions are full of references, which is quite unusual.

   We have elaborated the description of the aerosol-physics module SALSA in the revised manuscript and added references to articles where SALSA has been evaluated as follows:

   "Here we use SALSA to solve the aerosol microphysics. SALSA represents aerosols by dividing the aerosol size distribution into 10 size sections (or bins), where the aerosol population is further divided into a soluble and an insoluble sub-population. A detailed description of the SALSA size distribution given in Kokkola et al., (2018), elaborating on the size resolution and which aerosol compounds are treated in which size bin. In the same article, an evaluation of ECHAM-SALSA against satellite and ground based remote sensing instruments, in situ observations of aerosol composition and size distribution as well as aircraft measurements of aerosol composition has been performed. In addition, ECHAM-SALSA has been involved in several model experiments within the AEROCOM initiative, where models are compared against aerosol observations and each other (e.g. Burgos et al., 2020; Kristiansen et al., 2016; Kipling et al., 2016; Tsigaridis et al., 2014). Furthermore,

ECHAM-SALSA's capability to simulate aerosol-cloud interactions compared to satellite observations has been evaluated in a previous study by Saponaro et al., (2020)."

In addition, we have added references throughout the manuscript, where they were lacking.

3. P2L6-7: please provide a reference.

   We expanded the description on how BC affects climate in the introduction quite a bit and added references where they were missing.

4. P2L11-14: these two statements are redundant.

   The purpose of these two sentences was to explain how different emission sectors contribute to the total BC emissions in different parts of the globe. We re-formulated the sentences to make this more transparent.

5. P2L15: sea ice extent.

   corrected

6. P2L16-29: in this part of the introduction many protocols, documents and meetings are cited. However, any reference cannot be found. As a note, the whole section suffers from a general lack of peer-reviewed references.

   We added references to this part of the introduction as requested.

7. P4L14: replace "sections" with "bins" or "modes". Apply to all manuscript.

   We usually prefer "section" over "bin", but also have used "bin" in the past. "Modes" on the other hand is rather misleading as it usually used in modal aerosol models, which describe their aerosol size distribution in terms of log-normal modes. However, we comply with the referee and change from "section" to "bin".

8. P4L13-P5L9: I noticed here a tendency to oversimplification of processes. As examples: in which size mode sits BC or OC? Is OC considered to be completely soluble? The text can be kept simple, but more references should be provided, I assume Kokkola was not the only one using the model.

   We have re-written our description of the aerosol-physics module and added references throughout the text as mentioned above. Details of chemical compounds in different particles sizes in SALSA can be found in the model description and evaluation paper by Kokkola et al., 2018.

9. P5L2: what exactly it is meant with "all aerosol particles are assumed to have the same chemical composition"?

   Within one aerosol size bin, all aerosol compounds are assumed to be internally mixed, which means that in each aerosol particle in that size bin the mass fraction of each

compound is exactly the same. As aerosol compounds are also referred to as "chemical species", chemical composition makes sense to us.

10. P5L16: would this affect the DRE estimations for the 2030 and 2050 estimations? Could the author provide an estimate for this? I am particularly thinking of this publication doi:10.5194/acp-14-537-2014.

    This is a good point. As greenhouse gases heat the atmosphere, one can expect that many atmospheric processes are affected by this, for instance a warmer atmosphere can hold more water vapour, which may have strong cloud effects and thus affect aerosol concentrations. Furthermore, non-anthropogenic aerosol emissions might (e.g. biogenic emissions) may change. These effects are of course not accounted for when the greenhouse gas concentrations are held constant. We commented on this in the manuscript.

11. P6L20-23: no black line for SU in figure 2; I thought that CO2 emission was assumed to be the same for all simulations, why CO2 should then decrease? In what way a reduction of SU is unfavorable?

    We entirely re-wrote Section 3.1. As is obvious from the referee's comment, the discussion about CO2 leads only do misunderstandings and we therefore removed it. Just to clarify here: CO2 is one of the main focuses of the ECLIPSEv5a MITIGATION scenario which was used to construct our CLE scenario. However, as we do not consider changes in CO2 in our simulations (in fact, we fix the CO2 concentrations and don't deal with CO2 emissions at all), it was unnecessary to even mention CO2 here.
    As SU is generally attributed a cooling effect on climate, its removal would lead to warming. Therefore, when only thinking about climate alone (neglecting e.g. health effects), an SU emission reduction can be seen as unfavourable. The SLCP reduction scenarios have been constructed with this aspect in mind. We tried to explain this better in the text.

12. P6L27: I would call this increase as "negligible". Following a previous statement at L21"..OC and BC emissions are mostly unchanged. . ."

    We agree with the referee and changed the text accordingly.

13. P7L1-2: Why CLE-SU is compared with OC-SLCF? What do you want to demonstrate?

    Here we merely wanted to point out where the largest changes in emission strength "happen". As SU mainly comes from different sectors than BC and OC, the emission changes can also be seen between different scenarios / years. However, as stated above, we re-wrote Section 3.1 and hopefully made it less confusing.

14. P7L4-7: provide references and try to articulate a fluent story here.

    We added references to Winiger et al. (2019) and Sobhani et al. (2018).

15. P7L7-14: As also stated in P11L23, meteorology is very important and large-scale circulation and precipitation control the transport of pollutants to the Arctic. How do the

vertical structure of the atmosphere vary in your simulations? Is there any constant feature supporting your upper-lower atmosphere distinction (potential temperature, RH, temperature, etc. . .)?

The main process that controls the vertical distribution of emitted aerosol close to the source is wet deposition. This means that the aerosol concentrations due to local emission more or less continuously decrease until the cloud top is reached. All aerosol that is transported further up is either removed through the much slower processes of turbulent mixing or sedimentation, or it is transported away horizontally. As we are now talking about the stratosphere (above cloud), this horizontal transport is predominantly poleward. This is also how it works in ECHAM-HAMMOZ. In some sense one could say that the modelled average water cloud top defines the boundary between our defined lower and upper atmosphere (which, of course, depends on latitude as well). This can also be seen in Figure 5b (the CDNC values very quickly decrease above the blue dotted line) and the newly added Figure S5c in the supplement, which clearly shows that the cloud time fraction for water clouds is almost zero above that line.

16. P8F3: 1) How do your profiles in 2010 (F3) compare with observations? Are these simulations reasonable? Please elaborate in the text. If such profiles are off, all the following results in the manuscript will be biased. 2) Make use of literature to justify your results, there are plenty of studies on transport to the Arctic. 3) Please change the units from Kg/m3 to some more traditional units ug/m3.

    We added the following text to the manuscript

    " In Kokkola et al., 2018, the BC, OC, and SU vertical profiles modelled by ECHAM-SALSA were compared to several aircraft campaigns. There it was found that ECHAM-SALSA tends to overestimate BC concentrations in the source regions and underestimate BC concentrations at high latitudes. Furthermore, we compared the modelled BC vertical profiles to measurement data from the ATom and HIPPO campaigns (not shown), where the model compares quite well with the observations at all latitudes. The OC and SU modelled concentrations agreed in most cases much better with the observations."

    We changed the units in Figure 3 from kg/m3 to ng/m3.

17. P10F4: How are the burden calculated in F4? From F3 I would guess that BC burden would be higher in LA than in UP for at least 2010. But it appears to be the contrary. There is no consistency between units used in the text and in F4.

    The burdens are calculated as sum of the total mass of each species in each vertical layer that belongs either to the lower or upper part of the atmosphere as defined in the manuscript. Mathematically this can be written as
    *burden_spec = sum(c_spec(i)*dz(i)) ,*
    where i is the level index and dz(i) is the level height. The level height in ECHAM-HAMMOZ grows more or less exponentially with altitude, which makes it difficult to compare the total amounts of aerosol contained in different layers by looking at vertical profiles alone.
    We changed the units for BC in Figure 4 to reflect what was used in the text.

18. P12L21: “N100 are a common proxy for CCN”, never heard of it. Please provide a robust explanation and references.

    We added several references to the manuscript.

19. P12L23-26: along with the paper, there is a tendency to rapidly come to conclusions. I do understand that SU correlates well with N100, but here you do not bring any evidence of NPF dominating the SU concentrations. . .correlation does not always mean causation. Please explain this, potentially in 3.2.3.

    In the model, 97.5% of sulphur is emitted to the gas phase, so correlation between N_{100} and SU trends is a strong indication that the number concentration is very much controlled by how many new particles are formed by nucleation and then grown to N_{100} size through condensation of sulphuric acid to the particles, i.e. new particle formation (NPF) (e.g. Kerminen et al., 2018; Lee et al., 2019). We clarified this in the manuscript.

20. P13F5: N100 and CDNC both in 1/cm-3. Are the 2010 profiles similar to reality (see comment on F3)

    We changed the units for N_{100} in Figure 5.
    Cloud properties in ECHAM6.3-HAM2.3 (using the aerosol module M7) have been evaluated in Neubauer et al., 2019. ECHAM-SALSA uses the same tuning parameters and the model variables used as tuning constraints do not change much when switching from M7 to SALSA.
    Similarly, aerosol number concentration from ECHAM6.3-HAM2.3 (using M7) have been compared to observations in Watson-Parris et al., 2018 and found to agree fairly well. Direct comparison of ECHAM-SALSA N_{100} values with observations has not been performed yet, but are expected to be fairly similar.

21. P14L7 “A decrease in CDNC means that the cloud droplets are on average larger”. This is true if the liquid water content is constant, demonstrate the diameter change. Lower CDNC might mean

    We have added two figures to the Supplementary information that visualize this increase in cloud droplet size.

22. P18L26: Could you explain the difference between dry deposition and sedimentation?

    In this context, sedimentation is the mass flux due to the slow settling of aerosol particles, while dry deposition is the interception by features of the surface (rough surfaces, trees, buildings, etc.) of particles moving close to the surface. While both of these processes are usually combined into one term, in ECHAM-HAMMOZ they are stored in different outputs.

23. P20L19-24: Similar to aerosol vertical profiles. . .what are your aerosol concentrations in snow for the 2010 year, in the range of Doherty?

    As stated in the manuscript, ECHAM-SALSA does not track the BC concentrations in snow. If we would try to estimate a value in the way we did for the RF_{snow} values, this would be

merely based on the models used in Jiao et al. to simulate these quantities and would therefore not add any extra value to the manuscript.

Referee #3:

1. The introduction section seems heavily slanted towards the policy background to the study – while this is important, this section should include a little more of the scientific background on the climate and health impacts of aerosols and BC in particular, and how this study fits into the previous literature regarding global and regional-scale emission reductions.

   We extended the introduction to account for these shortcomings.

2. It's unclear how anthropogenic emissions that aren't directly tied to a country are treated in the scenarios – e.g. shipping emissions that occur over the ocean. Are reductions in these included in the mitigation scenarios, and if so, how are they included/excluded in the regional reduction scenarios like AC_ACT?

   This is a good point. For all emissions not covered by ECLIPSE we used the ECHAM-HAMMOZ standard inputs for year 2010. This includes, aircraft emissions, biogenic emissions, and wildfire emissions. Emissions from ships are included in ECLIPSEv5a, but have been held constant between the scenarios, because it is not clear how individual countries can affect these emissions. We added this information to the manuscript.

3. Throughout, the terms "lower atmosphere" (LA) and "upper atmosphere" (UA) are used to refer to the regions below and above 450 hPa. This is confusing, as the term "upper atmosphere" is commonly used to refer to much higher regions above the stratosphere and mesosphere (which are conventionally termed the "middle atmosphere"). I would recommend changing these to "lower troposphere" (LT) and either "upper troposphere" (UT, if contributions from the stratosphere and above are negligible) or "rest of atmosphere" (RA/RoA, otherwise).

   Thank you for this input. During writing the manuscript we have been struggling to find terms that reasonably well describe our 2-part division of the atmosphere and finally settled on LA and UA. The terms suggested by the referee are probably better (maybe not quite as catchy), so we decided to change our naming to "lower troposphere (LT)" and "rest of the atmosphere (RA)" as suggested.

4. p.5, lines 24–25 The MACC reanalysis only covers a period of 10 years, but these simulations are run for 30 years. Which year(s) of the reanalysis dataset are used for which years of simulation, or is a derived climatology used rather than the reanalysis directly? For future work, the authors should be aware that this dataset is now superseded by the CAMS reanalysis (Inness et al., 2019; 10.5194/acp19-3515-2019).

   Like with the greenhouse gas concentrations, we used the same values for all scenarios for all simulation years. The values chosen were the ones for 2010. In our model the O3 and OH concentrations only affect the oxidation of SO2 into sulfuric acid and hence only play a

minor role in this study. Nevertheless, we thank the referee for pointing this out and clarified this in the text. Also, recently the standard inputs to ECHAM-HAMMOZ have been changed from MACC to CAMS, and therefore the outdated oxidant fields are no longer in use.

5. p.6, lines 8–11 If the meteorology is fixed, then any changes in the source–receptor relationships arising from the rapid adjustments in the atmosphere will not be represented. The authors should consider briefly how significant the impact of this is likely to be.

   Good point. If meteorology in the model was not fixed, this would most likely affect the aerosol concentrations. However, we would expect the meteorology changes to mostly affect long-distance transport of aerosols. Health effects, on the other hand, are most noticeable inside or close to the source regions and we therefore think that our results would not change significantly. We elaborated on this in the manuscript.

6. p.12, line 24 Why must this be mostly NPF rather than the condensation growth of smaller particles to cross the size threshold?

   Here we consider the process of new particle formation to include both nucleation of new particles and their growth to CCN sizes (see e.g. Kerminen et al., 2018; Lee et al., 2019). We clarified this in the manuscript.

7. p.14, lines 1–2 As well as being "fairly small" this change is also not statistically significant given the stated uncertainty (especially in 2050; it's marginal in 2030).

   We tested statistical significance using the two-sided Mann-Whitney test (e.g. comparing two distributions of 30 yearly mean values). According to that test, the differences mentioned in the text are statistically significant.

8. p.14, line 16 Is this shift in vertical profile statistically significant or not?

   It is not. We changed the wording in the text to make this clear.

9. p.15, line 5 Since the error bars suggest the change in ERF is not statistically significant (unlike that in RF), it's stretching the data to say the changes "lead to warming" here.

   We tested statistical significance using the two-sided Mann-Whitney test (e.g. comparing two distributions of 30 yearly mean values). The change in the current legislation scenario between 2010 and 2030 and again between 2030 and 2050 is statistically significant. The difference between the different scenarios for the same year (e.g. CLE vs AC for 2030) are not statistically significant. We added this information to the manuscript.

10. p.23, line 18 "ECHAM" does not include prognostic aerosol; "ECHAM–HAM" or "ECHAM–HAMMOZ" should be used to refer to the aerosol–climate model.

    Agreed. We corrected this in the text.

11. p.24, lines 13–17 The model data used in the paper should be available to the reader (either from an archive, or at least by contacting the authors) without having to re-run the entire set of simulations.

    We agree. This has been an oversight from our part and we added the necessary statements to the data availability section.

12. Figures 3, 5 Can some indication of the uncertainty on these vertical profile differences be included, as has been done for some of the other types of plot? Otherwise it's unclear whether changes are statistically significant or not.

    We added a grey shading to all vertical profiles for the year 2010, which indicate the interval between the 10th and the 90th percentile of the data.

13. Figures 4, 6, 7, 8, 9 The manner in which the error bars represent uncertainty should be briefly stated in the caption.

    Good point. We added a statement to all captions.

Effects of Black Carbon Mitigation on Arctic Climate

Thomas Kühn[1,2], Kaarle Kupiainen[3], Tuuli Miinalainen[1], Harri Kokkola[2], Ville-Veikko Paunu[3], Anton Laakso[2], Juha Tonttila[2], Rita Van Dingenen[4], Kati Kulovesi[5], Niko Karvosenoja[3], and Kari E. J. Lehtinen[1,2]

[1]Department of Applied Physics, University of Eastern Finland (UEF), Kuopio, Finland
[2]Atmospheric Research Centre of Eastern Finland, Finnish Meteorological Institute, Kuopio, Finland
[3]Finnish Environmental Institute (SYKE), Helsinki, Finland
[4]European Commission, Joint Research Centre (JRC), Ispra (VA), Italy
[5]School of Law, University of Eastern Finland (UEF), Joensuu, Finland

Correspondence: Thomas Kühn (thomas.h.kuhn@uef.fi)

Abstract. We use the aerosol-climate model ECHAM-HAMMOZ to assess the effects of black carbon (BC) mitigation measures on Arctic climate. To this end we constructed several mitigation scenarios that implement all currently existing legislation and then implement further reductions of BC in a successively increasing global area, starting from the eight member states of the Arctic Council, expanding to its active observer states, then to all observer states, and finally to the entire globe. These scenarios also account for the reduction of the co-emitted organic carbon (OC) and sulphate (SU). We find that, even though the additional BC emission reductions in the member states of the Arctic Council are small, the resulting reductions in Arctic BC mass burdens can be substantial, especially in the lower troposphere close to the surface. This in turn means that reducing BC emissions only in the Arctic Council member states can reduce BC deposition in the Arctic by about 30 % compared to the current legislation, which is about 60 % of what could be achieved if emissions were reduced globally. Emission reductions further south affect Arctic BC concentrations at higher altitudes and thus only have small additional effects on BC deposition in the Arctic. The direct radiative forcing scales fairly well with the total amount of BC emission reduction, independent of the location of the emission source, with a maximum direct radiative forcing in the Arctic of about 0.4 W/m^2 for a global BC emission reduction. On the other hand, the Arctic effective radiative forcing due to the BC emission reductions, which accounts for aerosol-cloud interactions, is small compared to the direct aerosol radiative forcing. This happens because BC and OC containing particles can act as cloud condensation nuclei, which affects cloud reflectivity and lifetime, and counter-acts the direct radiative forcing of BC. Additionally the effective radiative forcing is accompanied by very large uncertainties that origin from the strong natural variability of meteorology, cloud cover, and surface albedo in the Arctic. We further used the model TM5-FASST to assess the benefits of the aerosol emission reductions on human health. We found that a full implementation in all Arctic Council member and observer states could reduce the annual global amount of premature deaths by 329000 by 2030, which amounts to 9 % of the total global premature deaths due to particulate matter .

1 Introduction

Black carbon (BC) is emitted into the atmosphere as microscopically small, solid particles formed as a result of incomplete combustion (Goldberg, 1985). The climate effects of atmospheric BC are complex. As an efficient light-absorbing compound it is generally thought to be warm the climate (Ramanathan and Carmichael, 2008). This effect becomes very important in the Arctic, because atmospheric light absorption is enhanced above the reflecting snow and ice surfaces, and also because the deposited BC particles darken the snow and ice, which affects the melt rate (AMAP, 2015). On the other hand, the aging of BC aerosol particles increases their hygroscopicity and makes them potential cloud condensation nuclei (CCN) (Kuwata et al., 2009). While increases in CCN will have a cooling effect, BC in cloud droplets or nearby clouds tends to warm the cloud, affecting the evaporation of clouds as well as the atmospheric stability, which leads to changes in cloud dynamics. This results in a semi-direct direct cooling effect (Koch and Del Genio, 2010). Eventually, as BC is deposited on snow and ice, it increases the melt rate and contributes to the thinning of glaciers and loss of arctic sea ice (Menon et al., 2010; AMAP, 2015). In addition, changes in BC emissions usually also affect the emission of other, co-emitted aerosol compounds, like organic carbon and sulphate (Klimont et al., 2017). These species mostly scatter light, therby reflecting part of the incoming sunlight, which leads to cooling (Kiehl and Briegleb, 1993). They also, like aged BC, can act as CCN and thus affect cloud properties (Twomey, 1977; Albrecht, 1989). Altogether this makes it very hard to assess the climatic effects of BC mitigation.

Apart from climate effects, aerosol mitigation is very important for enhancing air quality in many regions of the world, which affects many aspects of life, the most important of which is health. As humans (and animals) inhale aerosol (usually the measure is particulate matter with diameters below 2.5 µm or $PM_{2.5}$) for long periods of time, part of the aerosol mass deposits in the respiratory tract and may even enter the blood stream (Kim et al., 2015). This can severely increase the risk to develop many kinds of deseases, including respiratory deseases, heart deseases, and strokes (Pope III et al., 2002; Krewski et al., 2009; Anenberg et al., 2012). When assessing the importance of BC mitigation the co-benefits on these aspects should hence be taken into account (Partanen et al., 2018).

Emissions from within the Arctic area (which we here define as 60°-90° north), account for only a small fraction of the global emissions, and most of the impacts are induced by BC emitted and imported from outside the area (Winiger et al., 2019). Recent studies have indeed indicated that an important pathway of BC contributing to Arctic warming is through the transport of heated air masses from outside the area, especially from mid-latitudes (Yang et al., 2014; Sand et al., 2016).

Different emission sectors contribute differently to the total BC emissions in different parts of the world. Globally, burning of fossil fuels and biomass in transport, household heating, and cooking as well as wildfires are important emission sources of BC. In the Arctic Council member states, on the other hand, the key anthropogenic emission sources include transport and household heating as well as flaring in the oil and gas industry (AMAP, 2015; AMAP, 2019). Arctic shipping is currently a relatively minor source, but its relative importance is projected to increase with the decrease of the Arctic sea ice extent (Stohl et al., 2013).

The recent AMAP assessment (AMAP, 2015) indicated that with targeted choices of already existing mitigation measures of BC rich sources, it could be possible to cut the projected global and Arctic climate impacts significantly in the coming

few decades, provided that they could be implemented globally in a large scale. Such reductions can, however, be politically very demanding to achieve, since currently no mechanisms or policy processes are in place. At the international level, there are no legally binding mitigation measures applicable to BC, apart from commitments to reduce BC as part of fine particulate matter (PM 2.5) under the Gothenburg Protocol to the Convention on Long-Range Transboundary Air Pollution (United Nations, 1999). However, important non-binding processes to accelerate regional action exist under the Arctic Council. The key examples include the Framework document "Enhanced Black Carbon and Methane Emissions Reductions, An Arctic Council Framework for Action", adopted by the Arctic Council in their 2015 meeting (Arctic Council, 2015). According to the document, the Arctic Council member states are committed to accelerating the decline in BC emissions and call upon the Arctic Council observer States to participate in the efforts. Currently eight observer states have participated in the process. Furthermore, the 10th Arctic Council Ministerial Meeting in May 2017 adopted an aspirational collective goal of limiting BC emissions between 25 and 33 percent below 2013 levels by 2025 (Arctic Council, 2017). In addition to these non-binding formal frameworks, voluntary action can also be driven by co-benefits at the local scale, which include air quality, human health, and crop yields.

In this work we study what could be achieved by accelerated BC actions in the Arctic Council member states alone and together with the observer states in terms of reducing atmospheric burden, deposition and radiative forcing of BC in the Arctic. The analysis takes into account the cooling by co-emitted sulfur species and organic carbon. The results are compared with large-scale global emission reduction scenarios that have been the foundation of previous studies. The study brings to attention the unique and still relatively unexplored institutional potential of the Arctic Council to catalyze global regulatory action on the abatement of air pollution by engaging its observer states on concrete, quantitative and collective actions on BC reduction.

2 Methods

2.1 Emission Scenarios

As anthropogenic emission inputs we used the ECLIPSE version 5a emission scenarios, which include data for black carbon (BC), organic carbon (OC) or organic matter (OM), sulfur dioxide (SO_2), methane (CH_4), carbon monoxide (CO), nitrogen oxides (NO_x), non-methane volatile organic compounds (nmVOC) and ammonia (NH_3) from the IIASA-GAINS model (Stohl et al., 2015; Klimont et al., 2017). The emissions are available in five-year intervals, spatially distributed onto a $0.5°\times0.5°$ latitude grid, and include monthly data for the major sectors. For the present study, we only used emission data for the major aerosol compounds BC, OC, and SO_2, and re-gridded the data to the T63 model resolution, which roughly corresponds to $2°\times2°$.

We utilized particularly two of the scenarios, namely the Current Legislation (BASELINE) scenario and the short-lived climate forcer (SLCF) mitigation (MITIGATE) scenario, as starting point to construct the emission data sets for this study. The BASELINE scenario assumes that all 2015 agreed legislation and adopted policies affecting air pollutant emissions (see e.g. Cofala et al. 2007 and AMAP (2015)) will be implemented. The SLCF mitigation scenario (MITIGATE) additionally assumes the full global implementation of SLCF emission reduction technologies phasing in by 2030 and 2050 (see Shindell

Table 1. The Arctic Council member and observer states (before 2017).

Arctic Council members	Canada, Denmark, Finland, Iceland, Norway, Russia, Sweden, USA
Active observers	France, Germany, India, Italy, Japan, Poland, South Korea, Spain, United Kingdom
Other observers	China, the Netherlands, Singapore

et al. (2012)). The technologies were selected from existing emission control options for particulate and gaseous species in the GAINS model by assessing the potential climate impact using a climate metric (Shindell et al., 2012; Stohl et al., 2015) and can therefore be viewed as a maximum feasible SLCF reduction scenario.

For the purposes of this study we constructed combinations of the BASELINE and the MITIGATE scenarios to study the impact of emission reduction measures taken by the member states of the Arctic Council member and observer states (see Table 1 and Fig. 1) on the Arctic climate. As mentioned above, AMAP (2015) and Stohl et al. (2015) have used similar data sets, but they introduced the emission reductions globally whereas in this work we apply the emission reductions in successively larger regions of the globe. As a reference scenario we used the ECLIPSE BASELINE scenario (here referred to as CLE). We further constructed scenarios where the additional MITIGATE SLCF reductions are implemented (1) in the Arctic Council member states (AC), (2) in the Arctic Council member and active observer states (AC_ACT; countries that have shown interest in joining the Framework for Action on Black Carbon and Methane by submitting a national report to the Arctic Council in 2015), (3) in the Arctic Council member states and all observer states (AC_ALL), and (4) globally (GLOB; equal to the ECLIPSE MITIGATION scenario). The global extents of the implemented SLCF emission reductions for the different scenarios are outlined in Fig. 1. Ship emissions are included in the ECLIPSE scenarios, but it is unclear, how individual countries can affect these emissions and they are therefore the same in all scenarios. All emission data sets not covered by the ECLIPSE emissions (i.e. aircraft emissions, biogenic emissions, and wildfires) were taken from the ECHAM-HAMMOZ standard emission data sets (Granier et al., 2011; Diehl et al., 2012).

2.2 Aerosol-climate model

For our climate simulations, we used the aerosol-climate model ECHAM-HAMMOZ (ECHAM6.3-HAM2.3-MOZ1.0). The host atmospheric model ECHAM6 (Stevens et al., 2013) computes the atmospheric circulation and fluxes using a semi-Lagrangian transport scheme, HAM (Tegen et al., 2018) models aerosol processes, and MOZ (Schultz et al., 2018) (not used in this study) models atmospheric chemistry. Aerosol emissions, transport, radiation interaction, and water update are modelled with HAM. Within HAM, two different aerosol microphysics models can be used: either the modal aerosol module M7 (Tegen et al., 2018) or the Sectional Aerosol module for Large Scale Applications (SALSA) (Kokkola et al., 2018). Here we use SALSA to solve the aerosol microphysics (hereafter we refer to this model setup as ECHAM-SALSA) . SALSA represents aerosols by dividing the aerosol size distribution into 10 size sections (or bins), where the aerosol population is further divided into a soluble and an insoluble sub-population. A detailed description of the SALSA size distribution is given in Kokkola et al. (2018), elaborating on the size resolution and which aerosol compounds are treated in which size bin. In the same article, an

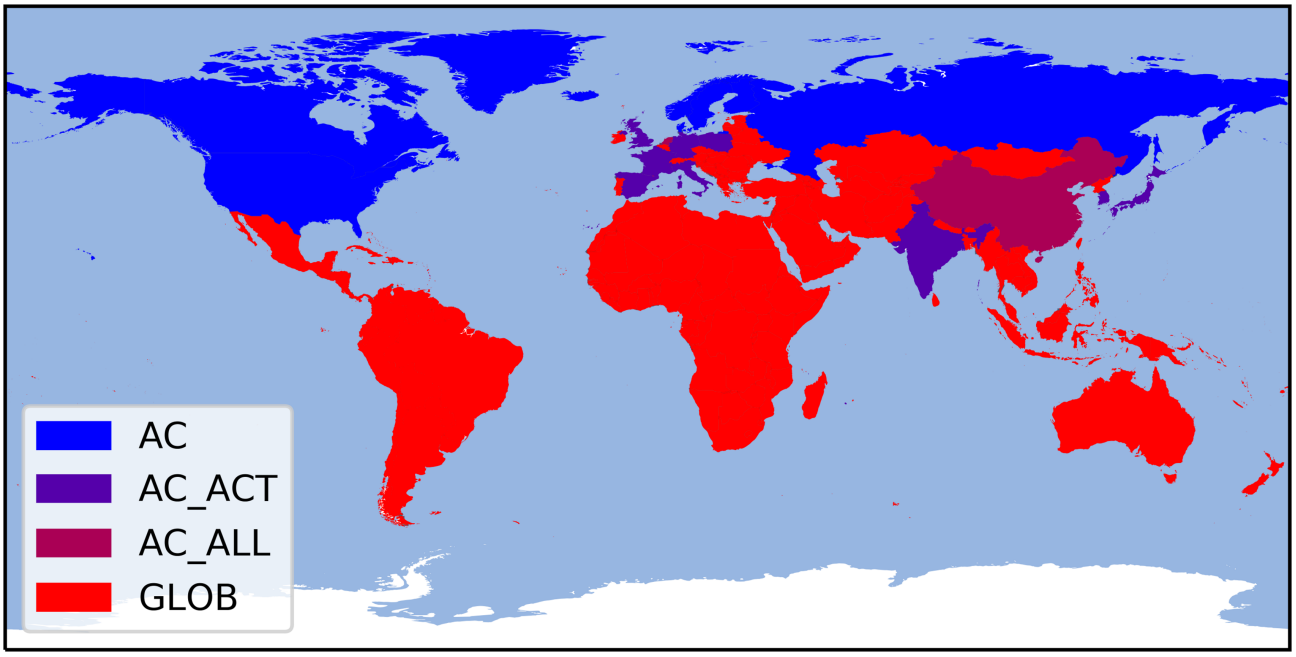

Figure 1. Global extend of SLCF reductions for the different scenarios. Starting from AC, each scenario includes all countries of the previous scenario (e.g. AC_ACT = AC plus active observer states).

evaluation of ECHAM-SALSA against satellite and ground-based remote sensing instruments, in situ observations of aerosol composition and size distribution as well as aircraft measurements of aerosol composition has been performed. In addition, ECHAM-SALSA has been involved in several model experiments within the AEROCOM initiative, where models are compared against aerosol observations and against each other (e.g. Burgos et al. (2020); Kristiansen et al. (2016); Kipling et al. (2016); Tsigaridis et al. (2014)). Furthermore, ECHAM-SALSA's capability to simulate aerosol-cloud interactions compared to satellite observations has been evaluated in a previous study by Saponaro et al. (2020). SALSA treats the chemical species sulphate (SU), organic carbon (OC), black carbon (BC), sea salt (SS), and mineral dust (DU). Within one size bin of one sub-population all aerosol particles are assumed to have the same chemical composition, while the two sub-populations are treated as externally mixed. SALSA solves the aerosol processes of nucleation, condensation, coagulation, activation into cloud droplets, and aerosol removal. HAM includes a simplified sulphate chemistry, which oxidises gaseous sulpuhr dioxide (SO_2) into sulphuric acid (H_2SO_4), which can either nucleate to form new particles or condense onto existing particles. 2.5 % of the total SO_2 emissions are converted into SO_4 at emission time and released as primary particles. In SALSA cloud droplet activation is solved using the parameterisation by (Abdul-Razzak and Ghan, 2002) such that both soluble and insoluble particles can form cloud droplets. In the cloud activation routine, SU and OC are treated as fully dissolved compounds, with hygroscopicity

values (κ) of 0.57 and 0.21, respectively. BC is assumed to be completely insoluble and contributes to cloud droplet activation only indirectly, by facilitating condensation of sulfric acid to the particle phase.

2.3 Climate simulations

The scenarios that were used in this study are outlined in Section 2.1. For each scenario, we considered the year 2010 to be the present, thus emission strengths are the same for all scenarios for 2010 and diverge after that. All SLCF emission reductions are assumed to be fully implemented by 2050 and we thus performed two simulations per scenario, one for the year 2030 and one for the year 2050. Together with the reference simulation for 2010, this makes a total of 11 simulations. In order to assure sufficient statistics, each simulation was run for 30 years plus half a year of spin-up.

As we here were only interested in assessing the aerosol effect on the Arctic climate, the atmospheric greenhouse gas mixing ratios were set to the values of the year 2010 for all simulations. The values used were based on the Representative Concentration Pathways 4.5 scenario (RCP4.5), following the fifth assessment report of the International Panel for Climate Change (IPCC) (IPCC, 2013) (note that for the year 2010 the greenhouse gas concentrations are almost identical for all four RCPs and therefore the choice of any particular RCP has no influence on the findings in this study). This means that the mixing ratios for CO_2, CH_4, and N_2O were set to 389.1 ppm, 1767 ppb, and 323 ppb, respectively. Furthermore, the sea surface temperatures (SST), sea ice cover (SIC), and (spatially varying) ozone concentrations were the same in all simulations. For SST and SIC we used the monthly varying climatologies from the PCMDI's Atmospheric Model Intercomparison Project (Taylor et al., 2012) for the year 2010. For the 3D ozone and OH concentrations we used the reanalysis of the atmospheric oxidants for year 2010 as described in Inness et al. (2013). It should be mentioned that fixing greenhouse gas concentrations, SST and SIC in this way prohibits several feedback mechanisms that may affect the magnitude of the simulated aerosol radiative forcing, mainly because atmospheric temperatures are not allowed to adjust freely. These effects include for instance changes in atmospheric water vapour content, which may affect clouds and thereby the atmospheric aerosol concentrations, and non-anthropogenic (e.g. biogenic) aerosol emissions, which may also affect the anthropogenic aerosol in several ways.

In all simulations performed in this study, the horizontal model resolution was set to the T63 spectral truncation, which corresponds to a resolution of roughly $2°\times2°$, and a vertical resolution of 47 hybrid sigma-pressure levels was used. The model meteorology was allowed to evolve freely. This, together with the fixed SST and SIC allows for rapid adjustments of the atmosphere while avoiding climate feedbacks and therefore makes it possible to calculate the effective radiative forcing (ERF) (Lohmann et al., 2010; Forster et al., 2016). The ERF is calculated as the difference of the average net radiative flux at the top of the atmosphere between the reference simulation (2010) and any of the simulations using emissions from a reduction scenario. The aerosol direct radiative effect (DRE) is calculated online by performing the radiation calculations twice, once with and once without accounting for aerosol-radiation interaction. The aerosol direct radiative forcing (DRF) is then again computed as the difference in DRE between the reference simulation (2010) and any of the simulations using emissions from a reduction scenario.

2.4 Human health and mortality evaluation

We utilized the Tracer Model 5 Fast Scenario Screening Tool (TM5-FASST), developed at JRC Ispra (Italy), to assess the impact of the different mitigation scenarios outlined in Section 2.1 on human health. TM5-FASST evaluates how air pollutant emissions affect large scale pollutant concentrations and their impact on human health (e.g. mortality and years of life lost) and crop yield. It utilizes source-receptor relationships to link emissions of pollutants in a given source region to downwind concentrations and related impacts. The source-receptor relationships have been derived by utilizing a large amount of simulations with the chemical transport model TM5 (Huijnen et al., 2010), which accounts for the effects of meteorology and chemical and physical processes on the transport of particulate matter (PM) (Van Dingenen et al., 2018). The source-receptor relationships were derived using present-day meteorological data and were fixed for all scenarios investigated here. Changes in aerosol concentrations can affect meteorology, which can feed back on certain aerosol processes, most noteably wet removal, and thereby transport of aerosol. By fixing the meteorology, these effects are effectively ignored. However, as aerosols have comparably short atmospheric lifetimes, aerosol sources affect PM surface concentrations close by the most and resulting error should therefore be relatively small. Health impacts from particulate matter with diameter smaller than 2.5 µm (PM2.5) are calculated as the number of annual premature mortalities from five causes of death, following the Global Burden of Diseases (GBD) methodology (Lim et al., 2012): ischemic heart disease, chronic obstructive pulmonary disease, stroke, lung cancer, and acute lower respiratory airway infections. More details on the model can be found in Van Dingenen et al. (2018).

3 Results

3.1 Global emissions

Figure 2 shows the change in the global anthropogenic emissions of black carbon (BC), organic carbon (OC), and sulphate (SU = SO_2+SO_4), which are the anthropogenic aerosol species that are modelled by ECHAM-SALSA. The first thing to note is the way that the different mitigation scenarios affect the aerosol emissions. The black line in each plot shows the effect of the current legislation (CLE) from year 2010 to 2050. Here SU shows the strongest changes in emission strength (about 19 % reduction by 2030), while OC and BC emissions change less (about 14 % and 13 % reduction by 2030, respectively). The SLCF mitigation scenarios include additional emission reduction measures to the CLE scenario for 2030 and 2050. As SU has an overall cooling effect in the atmosphere, it is usually considered unfavourable to reduce SU emissions when trying to slow global warming. Therefore, the SLCF mitigation measures have been selected such that they are mainly SU-neutral. In Figure 2 this can be seen by comparing the different scenarios for the same simulation year: while SU emissions show very little further change from the CLE scenario (less than 0.5 %; note how the lines in Fig. 2c lie on top of each other), BC emissions decrease dramatically, with a maximum reduction since 2010 of 81.3 % in 2050 for global implementation of the reductions (scenario GLOB). This amounts to decreasing the global anthropogenic BC emissions by 78.8 % in 2050 when comparing scenario GLOB to scenario CLE. As OC and BC are usually co-emitted species, the OC emissions decrease accordingly (70.7 % from 2010 to 2050 for scenario GLOB). Note in Fig. 2c how the anthropogenic emission strength of SU

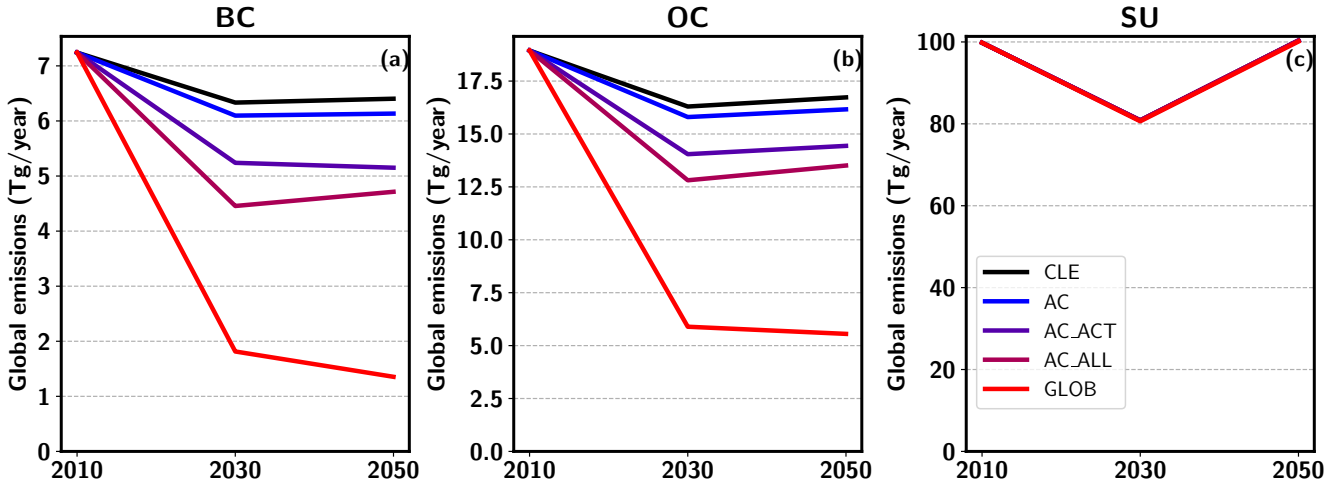

Figure 2. Total yearly global anthropogenic emission of BC (left), OC (middle), and SU (right) for the different emission scenarios. The colouring for the scenarios is the same as in Fig. 1, with CLE plotted in black.

almost recovers to the value of 2010 between 2030 and 2050, which can be attributed to economic growth. Here it should be noted that, while the global total emissions increase, regional trends, especially in the developed world (e.g. in Europe and Northern America), may be of opposite sign. In comparison, the changes in BC and OC emissions between 2030 and 2050 for the different emission scenarios are much smaller (and not necessarily of the same direction). This occurs because in the SLCF mitigation scenarios the mitigation measures are assumed to be fully implemented by 2030 and, furthermore, the largest part of BC and OC emissions come from different sectors than SU, which develop differently with time.

3.2 Arctic aerosol burdens

Depending on the emission site, pollutants can reach the Arctic through different transport pathways. While pollutants emitted within the Arctic are mostly transported close to the surface, pollutants from sources further south mostly enter the Arctic at relatively high altitudes (**?**Winiger et al., 2019). Uplifting of these pollutants happens either directly after emission or when the pollutants reach the polar dome. Within the polar dome, vertical exchange of air masses is very slow (Stohl, 2006; Quinn et al., 2011). In our simulations, this difference in transport pathways is clearly visible when analysing the vertical aerosol profiles over the Arctic region (60°-90° north). Figure 3a-c shows the Arctic yearly average vertical aerosol mass distribution profile for BC, OC and SU, respectively. All three profiles show two peaks as function of altitude – one close to the surface and one at approximately 200 hPa, which is above the Arctic tropopause. Each profile also shows a pronounced minimum between 400 and 500 hPa, depending on species. As the vertical location of aerosols within the troposphere is important for many atmospheric processes (e.g. aerosol-cloud interactions and aerosol deposition), we divided the Arctic atmosphere into a lower (LT) and an upper (RA) part, using the minimum of the BC profile (at approximately 450 hPa) as limit between the two. In Kokkola et al. (2018), the BC, OC, and SU vertical profiles modelled by ECHAM-SALSA were compared to several aircraft campaigns.

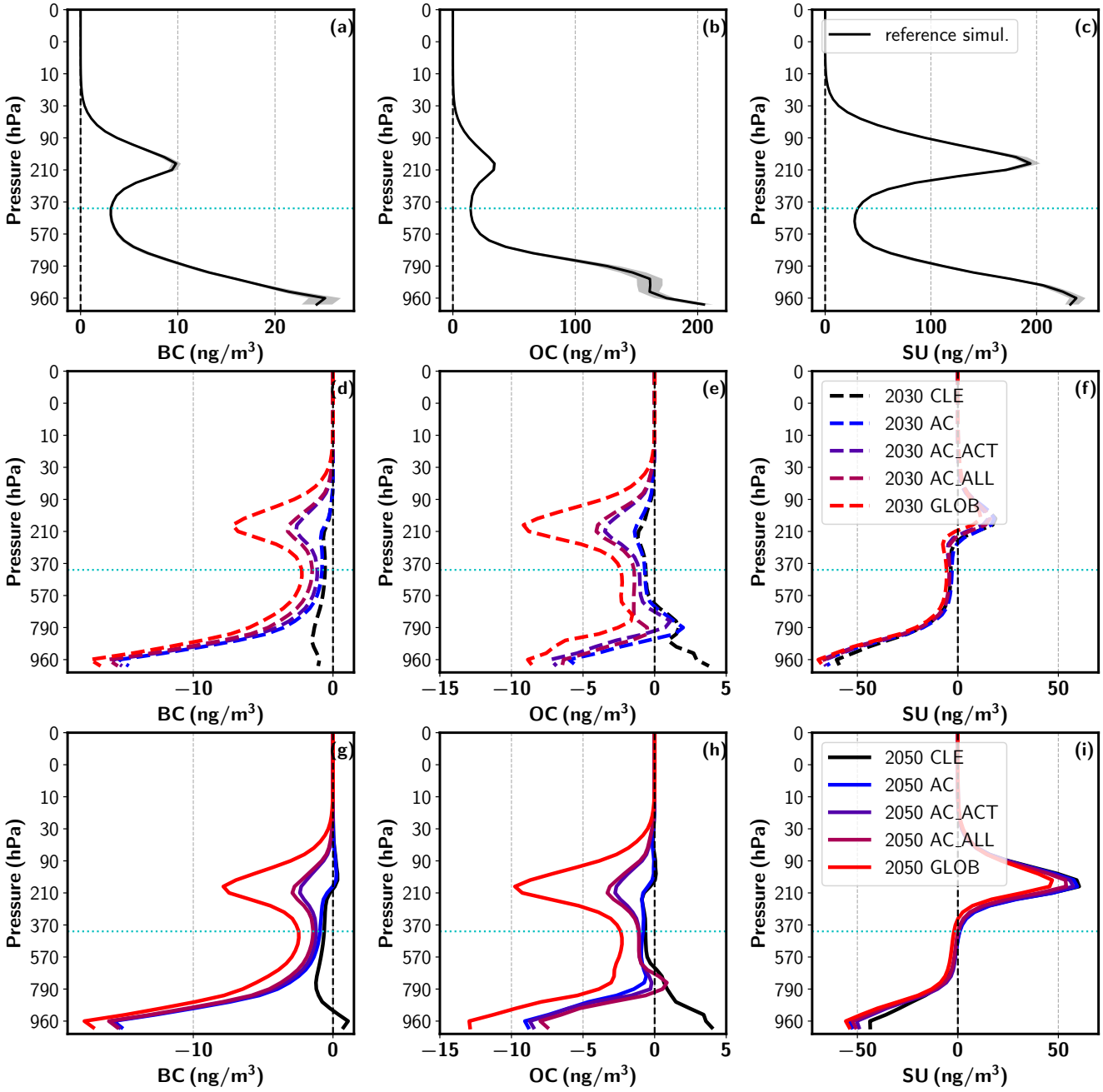

Figure 3. Arctic vertical profiles (top row) in 2010 and their respective changes in 2030 (middle row) and 2050 (bottom row) of BC (left column), OC (center column) and SU (right column). The grey shading in panels a – c denotes the interval between the 10^{th} and 90^{th} percentile of the data.

There it was found that ECHAM-SALSA tends to overestimate BC concentrations in the source regions and underestimate BC concentrations at high latitudes. Furthermore, we compared the modelled BC vertical profiles to measurement data from the ATom and HIPPO campaigns (not shown), where the model compares quite well with the observations at all latitudes. The OC and SU modelled concentrations agreed in most cases much better with the observations.

Figure 3d-f shows how the vertical profiles change from 2010 to 2030 for the different scenarios, while Figure 3g-i shows the changes from 2010 to 2050. As explained above, most of the aerosols emitted within the Arctic contribute to the LT concentrations. Accordingly, when reducing emissions in the Arctic Council member states (scenario AC), BC and OC concentrations decrease the most close to the surface, while the RA concentration changes are much smaller in comparison. When increasing the area of the SLCF mitigation, which mostly means emission reductions further south, the LT BC and OC concentrations show fairly little further decrease, while the RA concentrations begin to decrease noticeably.

As sulphate emissions are not very strongly affected by the SLCF mitigation, there are no big differences in concentration changes between the different scenarios (Fig. 3f and i) and most of the visible changes are due to the CLE emission changes. It is, however, noteworthy that SU concentrations react differently to the CLE emission changes than BC and OC do. While LT SU concentrations decrease, RA concentrations increase. This happens because in the model SU is mainly emitted as SO_2, which then is chemically processed to form SO_4 and finally partitions to the aerosol phase via new particle formation (NPF) and condensation to pre-existing particles. Note here that with NPF we denote the formation of new particles through nucleation of SO_4 and their concurrent growh to CCN sizes through further condensation of SO_4 onto these particles (Kerminen et al., 2018; Lee et al., 2019). Any shift in aerosol concentrations alters the condensation sink for SU and thus may affect the horizontal and vertical location of NPF. With a cleaner LT, more gaseous SU finds its way to the RA to undergo NPF there. The RA increase in SU concentrations is larger in 2050 than in 2030, because of increased SU emissions at lower latitudes.

Figure 4 shows the yearly average Arctic column burdens of BC, OC, and SU. Based on the earlier defined boundary between lower troposphere (LT) and rest of the atmosphere (RA) in the Arctic (approximately 450 hPa), we computed separate RA (Fig. 4a-c), LT (Fig. 4d-f), and total (Fig. 4g-i) column mass burdens for BC, OC, and SU, respectively. As may be anticipated from the global emissions, the SU mass burdens vary very little between the different scenarios and mainly follow the changes in time of the CLE scenario. The BC burdens show the strongest relative changes between the scenarios, while the relative OC burden changes are much smaller than the BC burden changes, but still larger than the SU burden changes. In the following we will analyse the different species separately.

3.2.1 Black carbon

In the CLE scenario, the yearly LT BC burden decreases by 11.7 ± 3.5 % (6.1 µg/m^2) and 9.6 ± 3.9 % (4.9 µg/m^2) for 2030 and 2050, respectively, compared to 2010. In contrast, the current legislation together with the SLCF reductions in the Arctic Council member states (AC scenario) reduce the LT BC burden of 2010 by 39.4 ± 3.9 % (20.4 µg/m^2) and 43.4 ± 3.6 % (22.5 µg/m^2) for 2030 and 2050, respectively. This means that the influence of BC emissions in the regions close to the Arctic on Arctic LT BC burdens is substantial. For instance, in 2030, the difference in global BC emissions between the CLE and AC scenarios is only −3.7 %, while the difference in yearly average LT BC burden is −31.3 %, which amounts to 14.3 µg/m^2. Comparing this to

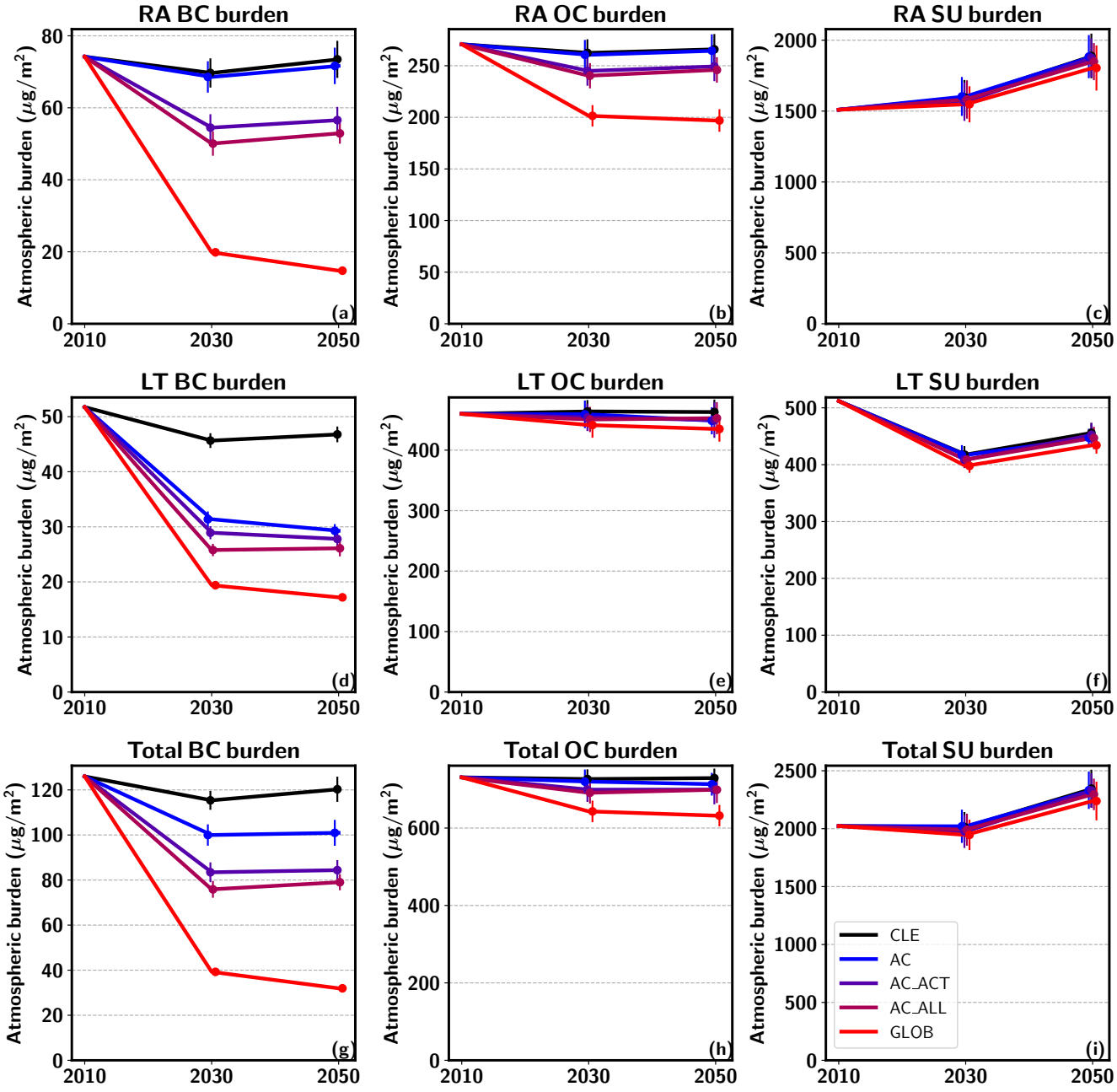

Figure 4. Arctic aerosol mass burdens for BC (left), OC (center), and SU (right). The top row shows the rest of the atmosphere (RA) burdens, middle row shows lower troposphere (LT) burdens, and bottom row shows the total column burden. The error bars show the standard deviation of the data.

a global SLCF reduction, the BC emissions in the same year decrease by 71.4 % between the CLE and GLOB scenarios, while the yearly average LT BC burden decreases by 57.5 % (26.3 μg/m^2). The AC_ACT and AC_ALL scenarios only induce small reductions in LT BC burdens compared to the differences between CLE, AC, and GLOB. Expressing this in terms of a burden reduction efficiency, which one may define as the ratio between the relative Arctic BC mass burden reduction and the relative global BC emission reduction, this would result in a LT burden reduction efficiency of 8.4 for the AC scenario and 0.8 for the GLOB scenario. This is an important result: while the potential in BC emission reductions in the Arctic Council member states may be small compared to the global total, the potential to decrease Arctic BC concentrations close to the surface is substantial.

Doing the same analysis for the yearly average Arctic RA BC burdens, the decreases in the CLE and AC scenarios since 2010 are fairly small (6.1 ± 8.6 % and 7.6 ± 8.9 %, respectively, for 2030). In fact, the variability in the change is larger than the actual simulated difference itself. Compared to the CLE scenario, the 2030 difference in RA BC burden in the AC scenario is −1.6 % (1.1 μg/m^2) and in the GLOB scenario it is −71.5 % (49.9 μg/m^2). AC_ACT reduces the RA BC burden by 15.2 μg/m^2 from AC, while AC_ALL makes only a small additional contribution. Using the same definition as above, the RA burden reduction efficiency is 0.3 for the AC scenario and 1.0 for the GLOB scenario. This means that emissions further south have a higher relative impact on RA BC burdens than emissions close to the Arctic (Note that even though the emission reduction regions in the different scenarios do not strictly expand north to south, the countries that add most of the emissions in each scenario are distributed that way).

In summary, Arctic BC burdens follow BC emission reductions very systematically: the lower the BC emissions, the lower the total Arctic BC burdens. However, emission sources close to the Arctic affect BC burdens in the lower troposphere much stronger than emission sources further south. The opposite is true for BC burdens in the rest of the atmosphere. As anthropogenic BC emissions at high latitudes are highest during the winter months and lowest during the summer, reductions in LT BC burdens are also strongest during the winter. The total LT BC mass burden, however, is higher during the summer months (but lower in the surface layer). The RA BC burdens do not show any seasonal trend.

3.2.2 Organic carbon

The yearly mean trends in Arctic OC burdens due to reductions in anthropogenic emissions largely follow the BC burden trends. However, while the absolute values of the changes are of the same order of magnitude for OC and BC, the relative changes in the OC burden are much smaller. This is due to the high contribution from natural sources (e.g. biogenic sources and wildfires) to the total OC emissions, which is most noticeable in the LT during the summer. For instance, in 2010 the Arctic LT OC burden during the summer months is on average 1341.1 μg/m^2, which is about 15 times more than the LT BC burden during the same period. In contrast, the LT OC burden in the winter months is only 86.1 μg/m^2, which is only about 1.6 times higher than the LT BC burden. The seasonal variation in the RA OC burden is much less dramatic (357.6 μg/m^2 and 226.8 μg/m^2 in the summer and winter, respectively).

Allowing the meteorology to evolve freely introduces considerable year-to-year variability in all transported species, because the wind and cloud fields have a relatively high natural variability, which affects both aerosol transport and removal. The variability in the mass burdens of any species is proportional to the total burden (due to both anthropogenic and natural

emissions). Because the emission reductions considered here only affect the anthropogenic contribution to the total burden, which for OC was already quite small to start with, this natural variability introduces fairly large uncertainties in the changes of atmospheric OC burdens. For instance in the CLE scenario, the change in Arctic LT OC burden from 2010 to 2030 during the summer months is 3.0 ± 8.1 %, which equals to $40.3 \pm 109.0\,\mu g/m^2$. In other words, the natural variability is more than twice the actual average change and more than the total LT BC burden. Relative to the CLE scenario, the changes in Arctic LT OC summer burden in 2030 due to BC mitigation amount to +0.7 % ($10.2\,\mu g/m^2$) and −1.7 % ($23.1\,\mu g/m^2$) for the AC and GLOB scenarios, respectively. In the winter the corresponding changes are −24.2 % ($-19.1\,\mu g/m^2$) and −40.4 % ($-31.9\,\mu g/m^2$), respectively. For the RA the changes show even higher variability, but are probably climatically not as relevant, as will be discussed below.

3.2.3 Sulphate

The changes in SU burden are qualitatively quite different from the changes in BC and OC burdens. Like BC and OC, the Arctic LT SU burden decreases in 2030 and 2050 compared to 2010, with the decrease in 2030 (about 18.4 ± 4.0 % for CLE) being larger than in 2050 (10.9 ± 4.3 % for CLE). In the upper troposphere, on the other hand, the SU burden increases by 5.8 ± 10.9 % and 25.1 ± 12.7 % in 2030 and 2050, respectively for the CLE scenario. This stronger increase in RA SU burden in 2050 compared to 2030 aligns well with the strong increases in SU emissions in India in 2050.

In general, the Arctic SU burden is largely unaffected by the SLCF reduction scenarios and appears to be dominated by the emission changes in the CLE scenario. However, there appears to be a slight trend of both the LT and RA SU burdens being lower with globally increasing coverage of the SLCF emission reductions. However, the uncertainties in these values are very big and especially the differences between the changes in different scenarios are much smaller than the accompanying uncertainties.

As has been discussed in the OC section above, the larger relative variability in SU burden changes can be explained by the relatively small change in total emission strength. While the anthropogenic SU emission reduction is the main driver for the average change in SU mass burden, the total SU emission strength (anthropogenic and natural) directly influences the magnitude of the variability of the change. Furthermore, both SU and OC have a higher water solubility than BC, which makes these substances more susceptible to aerosol-cloud interactions and wet removal, both processes being highly variable in the model.

3.3 Aerosol-cloud interactions

The discussed changes in aerosol concentrations have relatively strong effects on the cloud properties. Figure 5a shows the vertical distribution of the average concentration of aerosol particles with diameters larger than 100 nm (N_{100}) over the Arctic for the 2010 reference simulation. N_{100} is a commonly used proxy for the concentration of cloud condensation nuclei (CCN) (Dusek et al., 2006; Janssen et al., 2011; Tröstl et al., 2016). Figures 5d and 5g show the changes in the N_{100} profiles for 2030 and 2050, respectively. Here the influence of all aerosol species on N_{100} can clearly be seen. In the RA, the N_{100} trend appears to be dictated mainly by the SU trends. This indicates that the changes in RA N_{100} are mainly caused by changes in

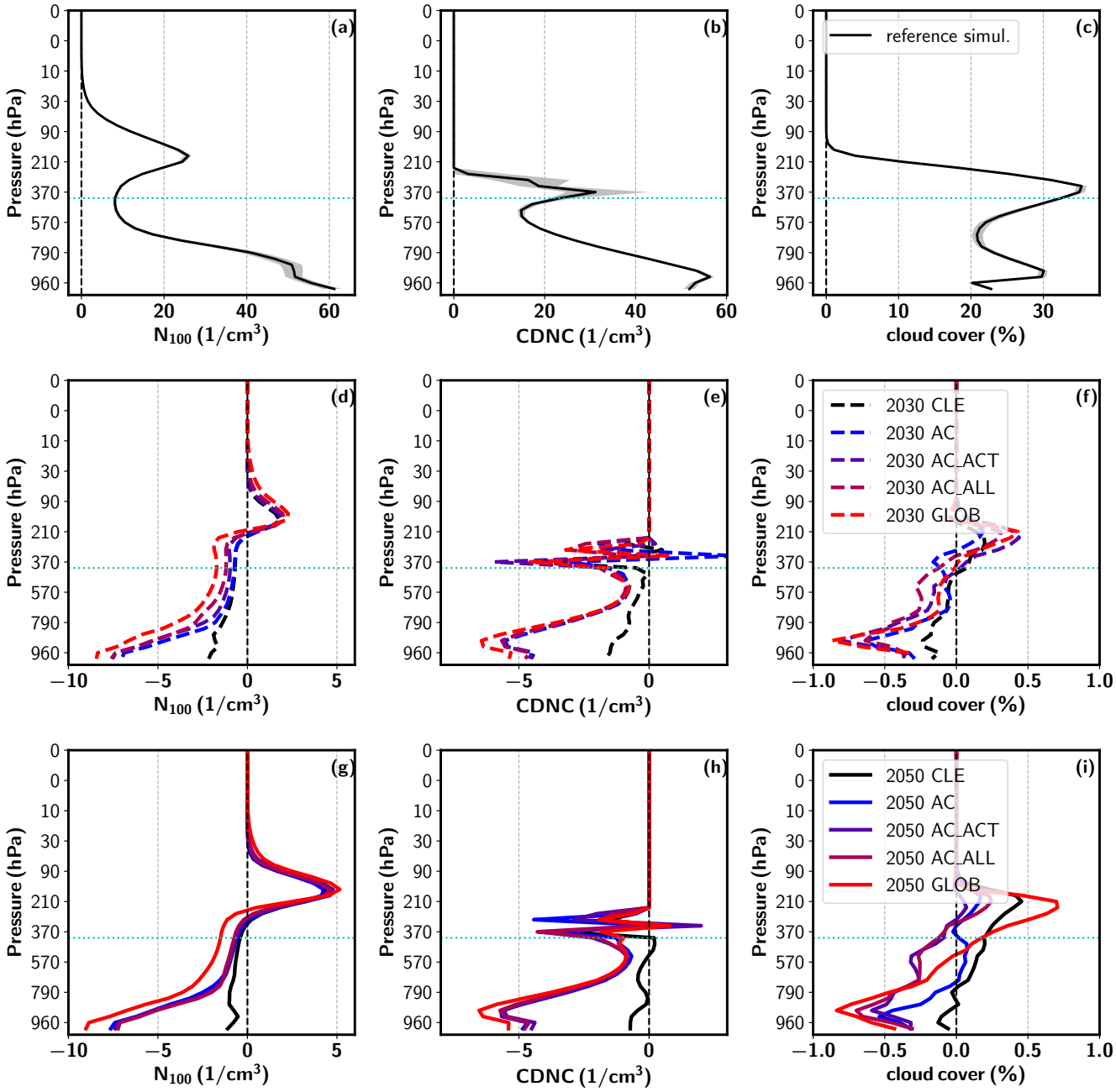

Figure 5. Arctic vertical profiles (top row) in 2010 and their respective changes in 2030 (middle row) and 2050 (bottom row) for N100 (left), CDNC (center), and cloud cover fraction (right). The grey shading in panels a – c denotes the interval between the 10^{th} and 90^{th} percentile of the data.

new particle formation (NPF). In the LT, on the other hand, the N_{100} trends appear to be more dependent on the BC and OC trends, especially close to the surface. This indicates that here changes in N_{100} are mainly governed by primary emissions. With our definition of the upper (RA) and lower (LT) atmosphere, in the CLE scenario the LT N_{100} burden decreases by 4.5 ± 5.5 % and 2.9 ± 5.7 % for 2030 and 2050, respectively, compared to 2010. For the AC scenario, the LT N_{100} burden decreases by 13.2 ± 5.5 % and 12.6 ± 5.5 % for the same years. As for the BC and OC mass burden trends, these changes are more pronounced during the winter months and are least distinguishable during the summer.

Figure 5b shows the yearly average vertical distribution of the Arctic cloud droplet number concentration (CDNC) for the 2010 reference simulation, while Figs. 5e and 5h show the respective changes for 2030 and 2050. Since most water clouds occur in the lower part of the atmosphere, we will restrict this discussion to LT CDNC. As may be expected, the changes in N_{100} affect the Arctic CDNC values. The change in LT CDNC burden since 2010 in the CLE scenario is fairly small: -3.5 ± 3.6 % in 2030 and -1.2 ± 3.4 % in 2050. The change in CDNC burden from the CLE to the AC scenario is -7.9 % and -10.0 % for 2030 and 2050, respectively, and varies only slightly for the other scenarios. This is in line with the LT OC and BC mass burdens changing most in the AC scenario, while the other SLCF scenarios affect the RA mass burdens more. Similar to the OC and BC mass burdens and the N_{100} burdens, CDNC burden changes are strongest during the winter and weakest during the summer.

A decrease in CDNC means that the cloud droplets are on average larger, which renders the clouds less reflective, amounting to a net warming effect (Twomey, 1977). For the scattering SU aerosols this means that the direct warming effects of SU reductions is amplified by the decrease in CDNC, while for the absorbing BC the reduction in CDNC counteracts the cooling effect of BC reductions. On the other hand, smaller CDNC values may accelerate precipitation formation, which in turn may shorten the cloud lifetime (Albrecht, 1989), which may reduce the cloud fraction. A reduced cloud fraction, depending on the conditions, may have either a warming or cooling effect. On one hand, if the cloud fraction is smaller, less sun light is reflected back to space, which nets to a warming of the atmosphere. On the other hand, less outgoing longwave radiation is reflected back to the surface, which nets to a cooling of the surface. The changes in Arctic cloud fraction will be discussed below in combination with the radiative forcings.

Figure 5c,f, and i indicate a small upward shift in the Arctic cloud cover vertical profile: the cloud cover fraction decreases in the LT and increases in the RA (this can also be seen in Figs. S5 and S6. However, these shifts are statistically not significant and we therefore do not investigate this further.

3.4 Radiative forcing

3.4.1 Global values

The global aerosol all-sky short-wave (SW) direct radiative forcing (sRF_A) is shown in Fig. 6a. The aerosol long-wave (LW) direct radiative forcing is an order of magnitude smaller than the SW forcing and will therefore not be discussed here. Omitting a detailed quantitative analysis, it can be seen that the sRF_A values very well reflect the emission reductions of the different scenarios: the more the BC emissions are reduced in any particular year, the larger the global cooling effect that can be seen

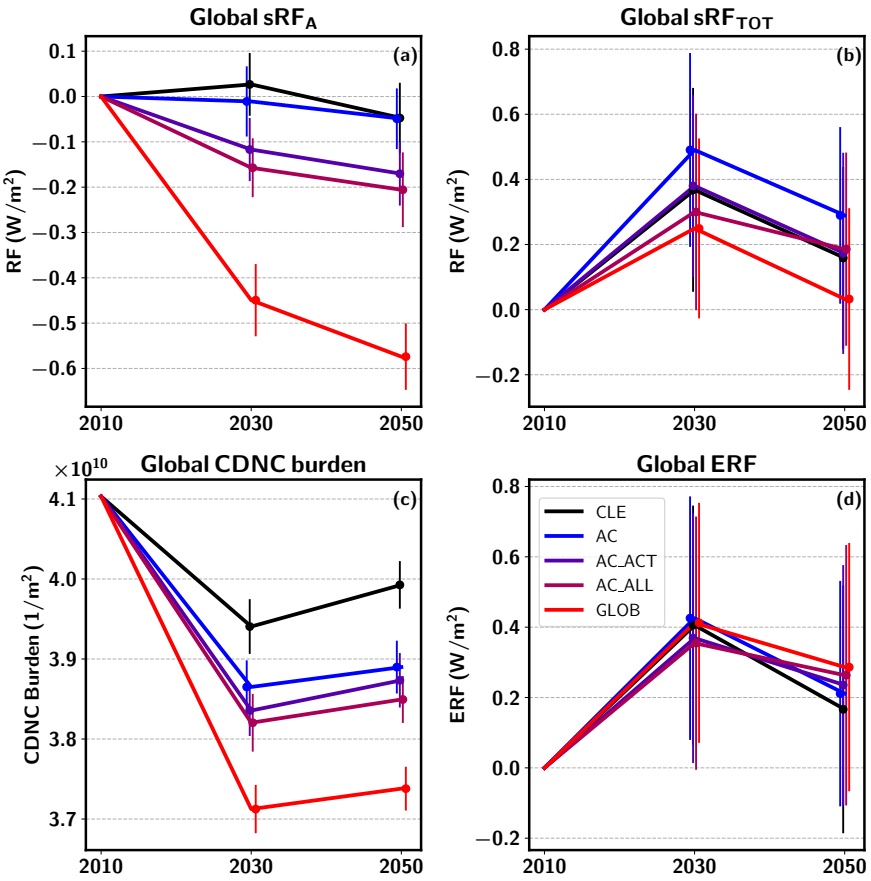

Figure 6. Global (a) direct short-wave aerosol radiative forcing , (b) total short-wave radiative forcing, (c) CDNC burden, and (d) effective radiative forcing. The error bars show the standard deviation of the data.

in the sRF_A values. A notable feature of the BC direct radiative forcing is that the BC all-sky forcing is typically larger (more negative) than the clear-sky forcing (not shown), which is opposite to the direct radiative forcings of scattering aerosols. This occurs because in a cloudy sky more sunlight is reflected back to space and thus the absolute amount of short-wave radiation leaving the planet is larger, which amplifies the light absorption effect of BC Samset and Myhre (2011); Kühn et al. (2014); Samset and Myhre (2015).

Compared to the sRF_A values of the SLCF scenarios, the sRF_A that is caused by the reductions in SU emissions in the CLE scenario is much smaller in magnitude. This can be seen by following the black line for the CLE scenario on Fig. 6a: Between 2010 and 2030, where global SU emissions decrease, the global sRF_A is slightly positive (0.03 ± 0.07 W/m^2), while between 2030 and 2050, where global SU emissions recover, the sRF_A is slightly negative (-0.05 ± 0.08 W/m^2). Altogether, a global implementation of the maximum feasible BC emission reductions (scenario GLOB) produces sRF_A values of -0.45 ± 0.08 W/m^2 and -0.57 ± 0.07 W/m^2 for 2030 and 2050, respectively, relative to the 2010 reference scenario. The

sRF_A values for the other scenarios follow the BC emission amounts fairly well. However, when taking also the indirect effects into account, the picture changes quite dramatically.

Figure 6b shows the total global short-wave radiative forcing (sRF_{TOT}; this quantity also includes rapid adjustments of the atmosphere to the changing aerosol emissions) at the top of the atmosphere. First off, the reduction in SU emissions in the CLE scenario between 2010 and 2030 produces a noticable, statistically significant warming signal of 0.37 ± 0.31 W/m^2, which decreases to 0.16 ± 0.28 W/m^2 in 2050, where the SU emissions almost recover to the value of 2010. On the other hand, the reductions in BC and OC in the SLCP scenarios compared to CLE indicate, depending on the scenario, either cooling or warming, with no visible systematic response to the amount of BC and OC reduction. However, the variability in sRF_{TOT} is considerable and the differences between different scenarios are statistically not significant. As the sRF_A values clearly are negative, this change in sign of the radiative forcing must be due to changes in planetary albedo, which may either be attributed to surface changes or changes in clouds. On the global average, the surface albedo (not shown) varies only slightly and may contribute to the variability in the radiative forcings, but cannot explain the difference between aerosol and total short-wave RF. We find, however, a strong effect in global average CDNC burdens (Fig. 6c). The amount of global average CDNC decreases very systematically with the amount of reduction in aerosol emissions. Here the effect of both SU reduction in the CLE scenario and BC and OC reduction in the SLCF scenarios are clearly visible. Between 2010 and 2030, the global average CDNC burden decreases by 3.5 ± 3.3 % from 3.7×10^{10}/m^2 to 3.6×10^{10}/m^2 in the CLE scenario, and the maximum reduction in CDNC due to SLCF reductions is 12.9 ± 2.9 % in 2030 between the CLE and the GLOB scenarios. The relation between CDNC and cloud radiative forcing has been studied in Storelvmo et al. (2009). They list the radiative forcings due to increases in CDNC at 950 hPa for different models. Interestingly, even though the CDNC base values and the CDNC increases vary a lot between models, the resulting radiative forcings are within 0.62 W/m^2 and 1.94 W/m^2. Using the values provided in Table 1 in Storelvmo et al. (2009), one can calculate a linear relation between percental CDNC change and cloud radiative forcing. The values range from -0.14 cm^3 W/m^2 for very low CDNC base values (41.9/cm^3) to -0.01 cm^3 W/m^2 for very high CDNC base values (158.7/cm^3). In the simulations performed here, we find an average cloud weighted CDNC at 940 hPa of 59.3/cm^3 with percental changes of up to 11.5 % in the SLCF mitigation scenarios. For these values, the difference between sRF_A and sRF_{TOT} that we observe can be explained with a factor between -0.05 cm^3 W/m^2 and -0.06 cm^3 W/m^2, which lies well in the range derived from Storelvmo et al. (2009). In addition to their ability to act as CCN, BC particles can also affect clouds through several semi-direct effects. As BC inside or close to clouds absorbs radiation, it can affect cloud droplet evaporation and atmospheric stability, which can also affect cloud properties and lead to cooling (Koch and Del Genio, 2010). These effects, however, are very difficult to distinguish from each other in ECHAM-HAMMOZ and are therefore not further diagnosed here.

There is also a decrease in cloud time fraction (fraction of the total simulated time that a grid box is in cloud) with decreasing aerosol emissions (not shown). The effect is fairly small, but the cloud time fraction does decrease systematically with the decreasing strength in aerosol emissions. In our simulations the decrease in cloud time fraction is most noticeable between the CLE and the AC scenarios and between the AC_ALL and the GLOB scenarios (the differences between AC, AC_act, and AC_all are very small). This implies that decreasing aerosol emissions close to very pristine environments has the biggest

effect on cloud time fraction. Generally a reduced cloud time fraction is attributed a warming effect, because the amount of reflected sun light back to space is reduced (Albrecht, 1989). However, at the same time the clouds also reflect less long wave radiation back to the surface (Ramanathan et al., 1989), which makes the effect on radiative forcings of this phenomenon less predictable. However, as the maximum change in cloud time fraction is only of the order of about 1 %, we reason that most of the effect of aerosol-cloud interactions on the radiative forcings is through the aerosol effect on CDNC.

Figure 6d shows the global effective radiative forcing (ERF), which is calculated as the difference in net radiation budget (SW and LW) at the top of the atmosphere (TOA) between the simulation scenarios and the 2010 reference scenario. For the CLE scenario the ERF is positive, amounting to 0.41 W/m^2 and 0.29 W/m^2 for 2030 and 2050, respectively, which is in line with the $\mathrm{sRF_{TOT}}$ values. This reflects quite well the global SU emission reductions, allowing for shifts in the location of the emissions. The differences between the different SLCF scenarios are very small and accompanied by very large uncertainties. This means that globally the direct radiative effects due to the BC emission reductions are counter-acted by cloud effects. This has also been reported in previous studis (Kuwata et al., 2009; Koch and Del Genio, 2010; Smith et al., 2018).

3.4.2 Arctic values

Figure 7a, d, and g shows the total Arctic aerosol direct radiative forcing ($\mathrm{RF_A}$, which includes both SW and LW radiation; note the difference to $\mathrm{sRF_A}$ discussed for the global forcings, which considers only SW radiation) for winter, summer, and all year, respectively. Like for the global values, the Arctic $\mathrm{RF_A}$ follows the BC burden reduction amounts very systematically with maximum $\mathrm{RF_A}$ values of −0.39 W/m^2 and −0.44 W/m^2 for 2030 and 2050, respectively, for the GLOB scenario. In a cloudy sky the RA BC concentrations contribute much stronger to the direct radiative forcing than the LT values (all BC mass below cloud is screened) Samset and Myhre (2011); Kühn et al. (2014); Samset and Myhre (2015). This is why the BC emission reductions of the Arctic Council member states have a relatively small effect on the $\mathrm{RF_A}$, which mostly cause lower-level changes in BC concentrations. Because of the strong seasonal cycle of solar insolation, the Arctic $\mathrm{RF_A}$ is much stronger during the summer than during the winter.

The Arctic ERF values (Fig. 7b, c, and h) principally follow the results obtained for the global ERF. However, here the relative uncertainty is even larger, taking values of the order of ±2 W/m^2. The ERF differences between the different scenarios are as high as 0.5 W/m^2, with no systematic ordering concerning the BC emission reduction strengths of the SLCF mitigation scenarios. Furthermore, the Arctic ERF values appear to be dictated quite strongly by the Arctic cloud cover (Fig. 7c, f, and i). In particular, the winter ERF and cloud cover have a strong positive correlation (0.80), while the summer ERF and cloud cover have a strong negative correlation (−0.97). This occurs, because during the winter, the long-wave warming of clouds dominates, while during the summer it is the short-wave cooling effect. In the yearly average, the correlation between ERF and cloud cover is much weaker (−0.64), because both short- and long-wave effects are important. This is also visible when comparing Figs. 7h and i.

The reason why $\mathrm{RF_A}$ and ERF are so different in the Arctic can be explained by cloud changes. During the winter, when BC and OC emission reductions in the AC scenario are largest, there is also a very strong decrease in LT CDNC burden (not shown) between the CLE and AC scenarios (21.4 %), while the differences between AC and the other SLCF mitigation scenarios are

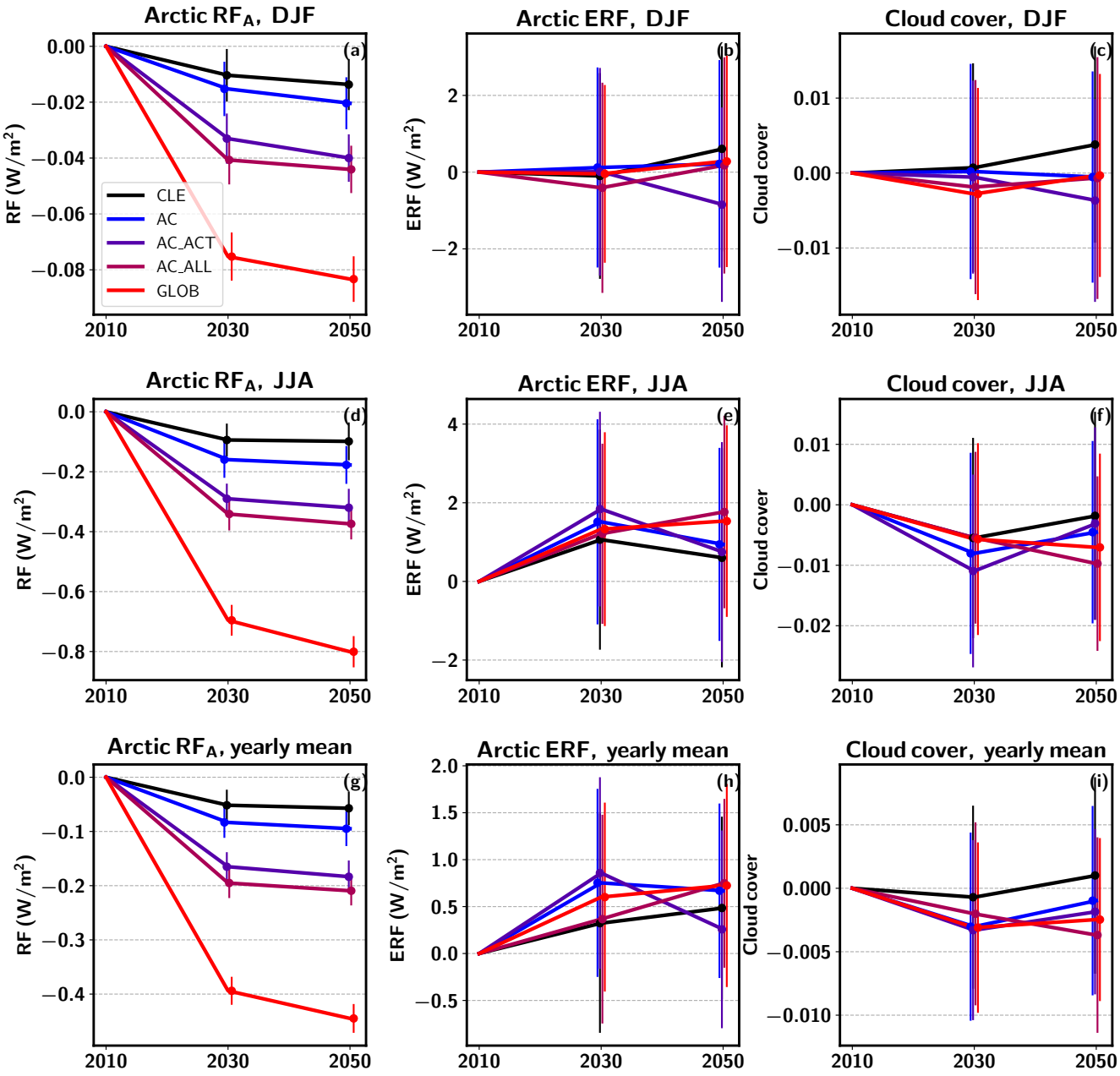

Figure 7. Arctic total aerosol all-sky direct radiative forcing (left), effective radiative forcing (center), and cloud cover (right) for winter (top), summer (middle), yearly (bottom) averages. The error bars show the standard deviation of the data.

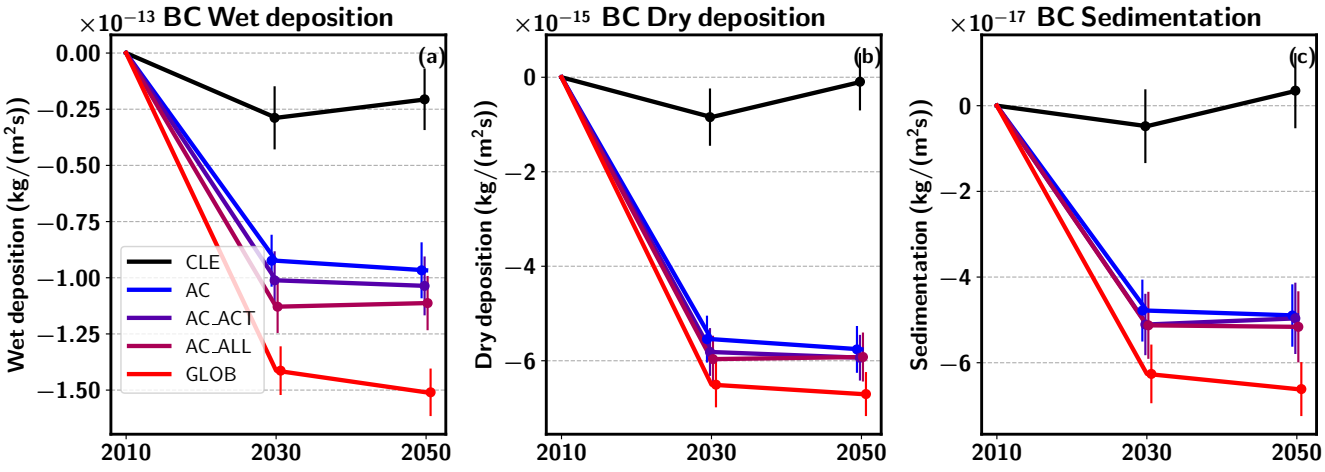

Figure 8. Arctic BC deposition fluxes: (a) wet deposition, (b) dry deposition, and (c) sedimentation. The error bars show the standard deviation of the data.

small, but systematic. During the summer the CDNC trends for the different scenarios are similar, but much less pronounced. Like for the global radiative forcings, we interpret the changes in Arctic CDNC as the main driver for the differences between RF_A and ERF.

As already mentioned, the Arctic ERF values show large uncertainties. The main contribution to these uncertainties are the strong natural variability in Arctic cloud cover and yearly average surface albedo, the latter of which is due to the year-to-year variability in snow cover. Other possible contributors are the variability in aerosol burdens, CDNC, and heat transport into the Arctic. Equally strong uncertainties in ERF have also been observed elsewhere (e.g. Cherian et al. (2017))

3.5 Surface

Deposition of BC on ice and snow is widely reported to strongly affect the surface albedo and accelerate snow and ice melt (Quinn et al., 2011; Bond et al., 2013; Sand et al., 2016). In ECHAM-HAMMOZ the deposition of BC is separated into wet deposition, dry deposition, and sedimentation, with wet deposition making the largest contribution to the total. As dry deposition is a function of the BC concentrations close to the ground and wet deposition only depends on in- and below-cloud BC concentrations, it is the LT BC concentrations that dictate the BC deposition rates in the Arctic. This can clearly be seen in Fig. 8: the LT BC burden reductions of the SLCF scenarios are directly reflected in the BC deposition rates. Even though the SLCF emission reductions in the Arctic Council member states, compared to the CLE scenario, only comprise 5.2 % and 5.3 % of the globally feasible total reductions, these reductions can reduce the Arctic BC deposition by 29.3 % and 33.8 % in 2030 and 2050, respectively. This comprises 57.8 % and 59.7 % of the achievable decrease in arctic BC deposition for global implementation of the SLCF emission reductions.

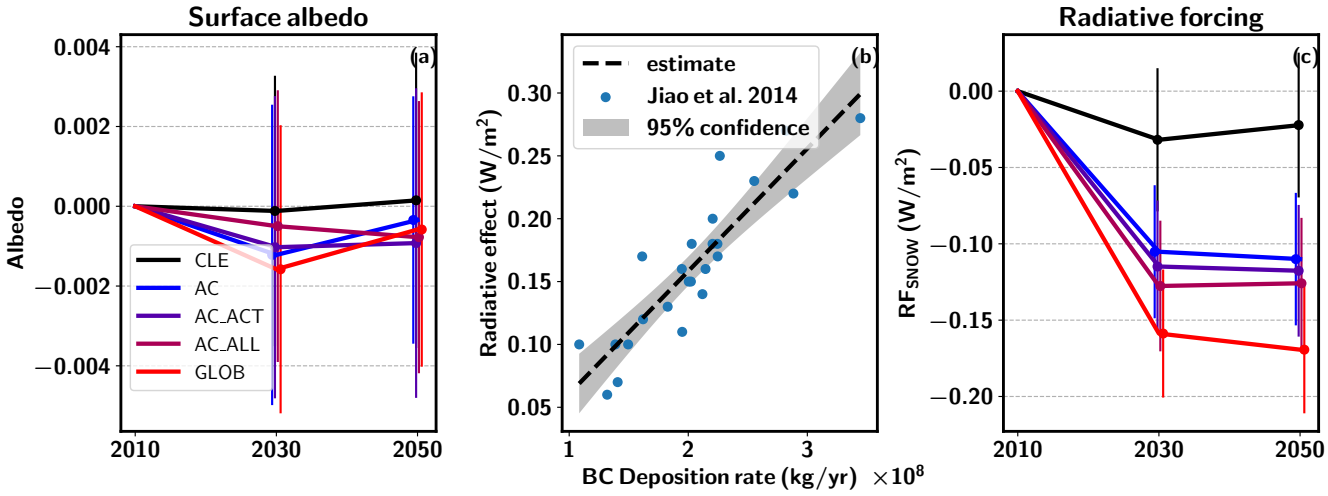

Figure 9. (a) Yearly average Arctic surface albedo, (b) linear regression to data from Jiao et al. (2014), and (c) Arctic surface radiative forcing to changes in BC deposition changes using results from (b). The error bars show the standard deviation of the data.

The Arctic surface albedo varies strongly during one year due to the big changes in snow and ice cover extent. Because the time that an area is covered by snow during one winter can change considerably from one year to another, the variations in yearly Arctic surface albedo are big as well (Fig. 9a). Surface albedo can take values between 0 and 1, and a change of 0.001 in surface albedo amounts to a change of 0.1 W/m^2 of sunlight absorption per 100 W/m^2 of solar insolation. As can be seen in Fig. 9a, the differences in average Arctic surface albedo between the scenarios can be up to 0.0012, with standard deviations of the order of 0.003. Note that in the simulations performed here the monthly varying sea ice extent was the same in each simulation and in each simulation year, which means that the variation in surface albedo is caused only by the varying snow cover.

Like many other climate models, ECHAM-HAMMOZ does not account for changes in snow albedo due to the deposition of absorbing aerosols. The effect of the modelled BC deposition flux on the Arctic snow albedo has been approximated for a wide selection of AeroCom (Aerosol Comparisons between Observations and Models) models in Jiao et al. (2014), which included also a previous version of the model used here, ECHAM5-HAMMOZ. There the modelled Arctic BC deposition fluxes were used as input to an independent surface model, which then computed the radiative effect due to the computed changes in surface albedo. In order to approximate the radiative forcings due to the changes in the Arctic BC deposition flux in this study, we used the data provided in Jiao et al. (2014) of all modelled Arctic BC deposition fluxes and the resulting radiative effects to derive a linear relationship between the two quantities. To this end, we performed an orthogonal distance regression (ODR) using the relationship $\mathrm{RE} = a \times \mathrm{F_{BC}} + b$, where RE is the Arctic radiative effect in W/m^2, $\mathrm{F_{BC}}$ is the yearly average Arctic BC deposition flux in kg/yr, and the coefficients a and b have the values $9.76 \pm 1.05 \times 10^{-10}$ W yr/(m^2 kg) and $3.69 \pm 2.21 \times 10^{-2}$ W/m^2, respectively. The regression is visualised in Fig. 9b. The fit shows that the remarkably linear

behaviour between BC deposition rate and RE, with relatively small standard deviations, even though we here used only yearly average fluxes, while Jiao et al. (2014) used monthly two-dimensionally resolved deposition fluxes as model input. This may, however, mainly be due to the fact that Jiao et al. (2014) used the same nudged meteorology for all simulations and only changed the prescribed BC deposition fluxes according to the models tested. The yearly Arctic BC deposition rates simulated here are well within the data range of the models used in Jiao et al. (2014).

Using the linear relation derived here, we computed the Arctic radiative forcings due to BC deposition (RF_{snow}) on snow and ice that may be expected for the simulations performed here (Fig. 9c). As may have been expected, the RF_{snow} values follow the BC wet deposition values ($F_{BC,wet}$) (Fig. 8a) very well, because of the linear relationship between F_{BC} and RF_{snow} and because wet deposition is the dominant BC deposition process. As emissions close to the Arctic contribute most to the LT BC burdens and thus have the biggest impact on Arctic BC deposition fluxes, these emissions also have a big influence on the RF_{snow} values. For instance, in 2030 RF_{snow} between CLE and AC is $0.07 \pm 0.04\,W/m^2$, more than half of the value obtained between CLE and GLOB, $0.13 \pm 0.05\,W/m^2$. For any given year, the absolute value of RF_{snow} increases with the amount of BC emission reduction, but the differences between AC, AC_act, and AC_all are fairly small. Considering the relatively small amount in BC emission reduction in AC compared to the other scenarios, the contribution of the BC mitigation of the Arctic Council member states to the Arctic RF_{snow} is quite substantial.

Jiao et al. (2014) remark that in the AeroCom models investigated there, the BC emission fluxes were constant in time, which is unrealistic, because BC emissions in some sectors (e.g. residential combustion and energy production) are higher during the winter and lower during the summer, especially at higher latitudes. According to them, this most likely leads to an underestimation of RF_{snow}, because less BC is deposited during the winter. As the albedo changes affect RF_{snow} most during the spring time, the winter is the most important period with respect to deposited BC affecting snow albedo. In the simulations performed in this study, we used the ECLIPSE emission scenarios, which provide a more realistic annual distribution of the emissions. Therefore the values for RF_{snow} would most likely be larger (in magnitude) if similar simulations would have been performed using the BC deposition fluxes modelled here. On the other hand, using monthly average BC deposition fluxes instead of deposition that is simultaneous with precipitation may overestimate RF_{snow} (Doherty et al., 2014). Altogether, to produce better estimates of RF_{snow}, an online snow and ice albedo model that accounts for BC deposition should be included. However, considering the large natural variability in snow cover (and thereby in surface albedo) in simulations with freely evolving meteorology, it may be equally challenging to extract Arctic RF values of that magnitude from such simulations as it is for RF due to atmospheric aerosol changes.

Comparing the Arctic RF_{snow} values to the Arctic ERF values, the latter of which differ at maximum by $0.4\,W/m^2$ and have standard deviations of the order of $0.5\,W/m^2$, the RF_{snow} values are relatively small. In fact, adding the surface snow albedo effect to the atmospheric ERF does not help to separate the total forcings into a meaningful or systematic order (not shown).

3.6 Human health

We used the number of premature deaths due to elevated concentrations of particulate matter as an indicator of the health benefits that can be achieved due to the emission reductions in the different scenarios. The health benefits of the emission

reduction of each scenario have been computed for each of the four regions defined in 1. Thereby we found that, compared to the current legislation (scenario CLE), emission reductions in the Arctic Council member states alone (scenario AC) reduces the amount of premature deaths by 30000 (19 %) and 41055 (23 %) in the Arctic Council member states in 2030 and 2050, respectively (Fig. S1). The additional health benefits outside the Arctic Council member states are relatively small. Globally the emission reductions in the Arctic Council member states prevent 33000 and 47000 premature deaths in 2030 and 2050, respectively (Fig. S4). In general, it can be said that the health benefits of the emission reductions are always largest in the region where the emissions are actually reduced (Figs. S1–S4). For instance, reducing emissions in the active observer states in addition to the Arctic Council member states increases the amount of prevented deaths within the active observer states from 43000 to 206000 in 2050. This means that even regions that do not directly benefit from the impact on Arctic climate still have a strong motivation to reduce their SLCF emissions. Globally, 329000 (9 %) premature deaths could be avoided in 2030 if the Arctic Council member states and all observer states would implement all SLCF mitigation options, which is 18 % less (403000 (11 %) avoided deaths) than for a full global implementation.

These estimates are smaller than, for example, in Anenberg et al. (2012), who estimated for a similar global mitigation scenario as the GLOB scenario used here that full implementation could annually avoid 0.6-4.4 million premature deaths globally in 2030. We acknowledge that the overall particulate matter (PM) concentrations contain also other species, e.g. ash and secondary material from atmospheric transport, which is why this estimate is a conservative one and should be seen as a demonstration of the magnitude of the effects rather than a full analysis of PM related health effects. Furthermore, due to the coarseness of the models used here (and global models in general), concentration spikes (both spatial and temporal) cannot be simulated to their full extent, which lessens the overall impact of PM concentrations on human health. Another reason for the discrepancy is probably the different exposure-response function used, which in TM5-FASST flattens off at higher PM2.5 concentrations. However, as all these shortcomings are true for both the reference scenario (CLE) and the mitigation scenarios, the relative changes in premature deaths contain valuable information nonetheless.

4 Conclusions

In order to assess the impacts of black carbon (BC) mitigation policies on Arctic climate, we studied the radiative forcings that occur when such policies are applied. To this end, we constructed emission scenarios using the fairly recently published ECLIPSE v5a emission scenarios (Stohl et al., 2015; Klimont et al., 2017). The scenarios were constructed such that they reflected the full implementation of all currently agreed policies and furthermore implemented the maximum feasible BC mitigation in a successively increasing area of the globe, including the Arctic Council member states, Active observer states, all observer states, and finally the entire globe. The different geographical extents for mitigation were studied because of the extensive work that has already been done by the Arctic Council regarding BC mitigation measures and the large interest in its member states to actually reduce BC emissions. The probability that the emission reductions will be implemented in part or all of the areas defined in 1 is therefore relatively high. Thus studying these scenarios is very timely and important. The scenarios

account for the simultaneous decrease of co-emitted species. We restricted this study to the radiative forcings due to changes in aerosol emissions. In particular greenhouse gas concentrations were the same in all simulations.

We found a very strong relation between total global reduction in anthropogenic BC emissions and Arctic BC mass burdens. Similar relations were also found for organic carbon (OC) and sulphate (SU), but for these species the natural background is much larger and thus the changes in Arctic burden are of less relative importance. As reported in elsewhere (Stohl, 2006; Quinn et al., 2011), we find that emissions close to the Arctic influence more the BC concentration near the surface, while emissions further south mainly control the BC concentrations at higher altitudes. We here divided the Arctic BC mass burdens into a lower troposphere (LT) and an rest of the atmosphere (RA) contribution and found that, even though the maximum feasible reductions in BC emissions in the Arctic Council member states are small compared to the global potential, the effect that these reductions have on the LT BC burdens are considerable. This is very important, because the LT BC burden has a very strong influence on Arctic BC deposition to the surface, while the RA BC burden affects BC deposition only slightly.

We find a fairly linear relationship between Arctic BC and OC burden and Arctic direct aerosol radiative forcing (RF_A), independent on the altitude at which the BC concentration changes. BC and OC are usually attributed opposite effects on direct radiative forcing and cannot really be separated here, because the changes in BC and OC burdens are so similar in the different scenarios. However, due to the extensive masking by clouds in the Arctic, the OC effect is expected to be much smaller than the BC effect. There is no discernible effect of SU on Arctic RF_A.

In contrast to the RF_A, the Arctic effective radiative forcing (ERF) (Lohmann et al., 2010; Forster et al., 2016) shows no noticeable trend as function on BC or OC burden and the ERF values are accompanied by very large uncertainties. We argue that the RF_A contribution to the ERF is cancelled by changes in cloud droplet number concentrations (CDNC) and cloud cover (Twomey, 1977; Albrecht, 1989; Storelvmo et al., 2009). The uncertainties in the ERF are due to the strong natural variations in the model meteorology, which ultimately causes variations in CDNC, cloud cover, surface albedo, and, possibly, energy transport into the Arctic. Similar uncertainties in Arctic ERF have also been reported in other studies (Cherian et al., 2017). Our model does not account for snow albedo changes due to BC deposition. We therefore tried to estimate the resulting radiative forcing (RF_{snow}) in our simulations with the help of results from another study (Jiao et al., 2014). We found that the RF_{snow} due to the simulated BC emission reductions may be relevant, but would still be small compared to the uncertainties in snow cover fraction and ERF that we encountered.

The potential of BC mitigation to achieve a slowing of Arctic warming on a relatively short time scale has been discussed widely in the literature (Quinn et al., 2011; Bond et al., 2013; Jiao et al., 2014; Samset and Myhre, 2015; AMAP, 2015; Cherian et al., 2017). BC is a good candidate for this very important goal because of its strong interaction with solar radiation. However, as was shown in this study, conclusions about the efficacy of BC mitigation measures cannot be based on the direct effects of BC-radiation interactions alone. Instead also co-emitted species and aerosol-cloud interactions have to be taken into account. According to the fifth assessment report of the IPCC (Stocker et al., 2013), aerosol-cloud interactions contribute the largest amount of uncertainty to radiative forcing estimates and climate projections in climate models. These uncertainties arise due to differences in different climate models, with ECHAM-HAMMOZ and especially ECHAM-SALSA having a stronger-than-average aerosol-cloud coupling (Smith et al., 2018). It may therefore well be that using the same scenarios used in this study,

another model would predict more cooling. The uncertainties in ERF reported here are due to model-internal variability. Here we used 30 integration years for our simulations, which is recommended for ERF values of at least 0.1 W/m^2 (Forster et al., 2016). As the area studied here is relatively small and the Arctic surface albedo and cloud cover are highly variable already, it may be possible that much longer integration times are needed in order to obtain conclusive results, if the Arctic ERF is small. This may, however, be computationally too costly. Other methods to estimate the ERF have been suggested (Forster et al., 2016), which may reduce variability, but often suppress important climate-relevant processes, like, for instance, the effects of changes in meteorological conditions on cloud dynamics (Forster et al., 2016; Zhang et al., 2014). It may therefore be necessary to develop alternative methods to quantify climate effects in the Arctic. Finally, estimating climate impacts by computing the ERF due to a given change in emissions will never draw the entire picture, because fixing the sea surface temperature (SST) and sea ice cover (SIC) prohibits important climate feedbacks, like, e.g., changes in the oceanic heat transport into the Arctic and the resulting changes in SST and SIC, changes in precipitation, and accelerated snow melt. All these feedbacks affect Arctic surface temperatures in addition to the ERF and it may therefore be better to use a fully coupled ocean-aerosol-climate model to estimate Arctic temperature responses to changing aerosol emissions.

In addition to the climate impacts, reducing BC emissions also has positive effects on human health. Using the model TM5-FASST (Huijnen et al., 2010; Van Dingenen et al., 2018) we found that globally 329000 and 402000 premature deaths could be prevented by 2030 and 2050, respectively, if the proposed emission reductions (Stohl et al., 2015; Klimont et al., 2017) would be fully implemented in all Arctic Council member and observer states. Compared to other studies (Anenberg et al., 2012) this is a conservative estimate, because we only considered part of all fine particulate matter (PM2.5) in this study.

To conclude, even though the direct radiative effect of BC mitigation is easily quantifiable, the accompanying aerosol-cloud interactions of BC and its co-emitted species are still highly uncertain. Together with the natural variability of surface albedo and meteorology, this makes the overall effect on Arctic climate hard to assess. This does, however, not mean that BC mitigation is not useful in slowing Arctic warming, especially considering that several climate feedbacks that are not considered here (e.g. snow albedo feedback and BC effects on cloud dynamics) may further increase the BC warming potential. Further studies, including more models, will be needed in order to obtain higher-confidence estimates of the efficacy of BC mitigation strategies.

Code availability. The ECHAM6-HAMMOZ model is made available to the scientific community under the HAMMOZ Software Licence Agreement, which defines the conditions under which the model can be used. The licence can be downloaded from https://redmine.hammoz.ethz.ch/attachm HAMMOZ_June2012.pdf

Data availability. The model data can be reproduced using the model revision r5888 from the repository https://redmine.hammoz.ethz.ch/projects/hammoz show/echam6-hammoz/branches/fmi/white (last access: 24. Sep 2019, HAMMOZ consortium, 2019). Alternatively, the data can be obtained directly from the authors. The settings for the simulation are given in the same repository, in folder https://redmine.hammoz.ethz.ch/projects/hammoz/repos

hammoz/branches/fmi/acp_2019_09_24_settings. The ECLIPSE emission input files are available from http://www.iiasa.ac.at/web/home/research/research All other emission input files are ECHAM-HAMMOZ standard and are available from the HAMMOZ repository (see https://redmine.hammoz.ethz.ch/proj

Author contributions. TK and KK designed the outline of the paper. TK and KK wrote the majority of the paper. TK performed all climate simulations. VVP and KK generated the emission scenarios for the climate simulations. TK, TM, HK, AL, JT, and KEJL performed the data analysis for the climate simulations and produced the figures. RVD performed the FASST simulations. VVP, KK, and RVD performed the TM5-FASST data analysis. All authors contributed to the writing of the paper.

Competing interests. The authors declare that they have no conflict of interest.

Acknowledgements. This work was supported by the Academy of Finland projects WHITE (grant no. 286613), RECON (grand no. 308292), NABCEA (grant no. 296644), and the Centre of Excellence (grant no. 272041). The authors wish to acknowledge the CSC-IT Center for Science, Finland, for computational resources. The ECHAM-HAMMOZ model is developed by a consortium composed of ETH Zürich, Max Planck Institut für Meteorologie, Forschungszentrum Jülich, University of Oxford, the Finnish Meteorological Institute and the Leibniz Institute for Tropospheric Research, and managed by the Center for Climate Systems Modeling (C2SM) at ETH Zürich.

References

Abdul-Razzak, H. and Ghan, S. J.: A parameterization of aerosol activation 3. Sectional representation, Journal of Geophysical Research: Atmospheres, 107, AAC 1–1–AAC 1–6, https://doi.org/10.1029/2001JD000483, https://agupubs.onlinelibrary.wiley.com/doi/abs/10.1029/2001JD000483, 2002.

Albrecht, B. A.: Aerosols, Cloud Microphysics, and Fractional Cloudiness, Science, 245, 1227–1230, https://doi.org/10.1126/science.245.4923.1227, https://science.sciencemag.org/content/245/4923/1227, 1989.

AMAP: AMAP assessment 2015: Black carbon and ozone as Arctic climate forcers, 2015.

Anenberg, S. C., Schwartz, J., Shindell, D., Amann, M., Faluvegi, G., Klimont, Z., Janssens-Maenhout, G., Pozzoli, L., Dingenen, R. V., Vignati, E., Emberson, L., Muller, N. Z., West, J. J., Williams, M., Demkine, V., Hicks, W. K., Kuylenstierna, J., Raes, F., and Ramanathan, V.: Global Air Quality and Health Co-benefits of Mitigating Near-Term Climate Change through Methane and Black Carbon Emission Controls, Environmental Health Perspectives, 120, 831–839, https://doi.org/10.1289/ehp.1104301, https://ehp.niehs.nih.gov/doi/abs/10.1289/ehp.1104301, 2012.

Bond, T. C., Doherty, S. J., Fahey, D. W., Forster, P. M., Berntsen, T., DeAngelo, B. J., Flanner, M. G., Ghan, S., Kärcher, B., Koch, D., Kinne, S., Kondo, Y., Quinn, P. K., Sarofim, M. C., Schultz, M. G., Schulz, M., Venkataraman, C., Zhang, H., Zhang, S., Bellouin, N., Guttikunda, S. K., Hopke, P. K., Jacobson, M. Z., Kaiser, J. W., Klimont, Z., Lohmann, U., Schwarz, J. P., Shindell, D., Storelvmo, T., Warren, S. G., and Zender, C. S.: Bounding the role of black carbon in the climate system: A scientific assessment, Journal of Geophysical Research: Atmospheres, 118, 5380–5552, https://doi.org/10.1002/jgrd.50171, https://agupubs.onlinelibrary.wiley.com/doi/abs/10.1002/jgrd.50171, 2013.

Cherian, R., Quaas, J., Salzmann, M., and Tomassini, L.: Black carbon indirect radiative effects in a climate model, Tellus B: Chemical and Physical Meteorology, 69, 1369 342, https://doi.org/10.1080/16000889.2017.1369342, https://doi.org/10.1080/16000889.2017.1369342, 2017.

AMAP: EU-funded Action on Black Carbon in the Arctic, 2019. Review of Reporting Systems for National Black Carbon Emissions Inventories: EU Action on Black Carbon in the Arctic – Technical Report, 2019.

Arctic Council: Annex 4. Iqaluit 2015 Sao Report To Ministers. Enhanced Black Carbon And Methane Emissions Reductions An Arctic Council Framework For Action., https://oaarchive.arctic-council.org/handle/11374/610, 2015.

Arctic Council: Expert Group on Black Carbon and Methane; Summary of Progress and Recommendations, https://oaarchive.arctic-council.org/handle/11374/1936, 2017.

Burgos, M. A., Andrews, E. J., Titos, G., Benedetti, A., Bian, H., Buchard, V., Curci, G., Kirkevåg, A., Kokkola, H., Laakso, A., Lund, M. T., Matsui, H., Myhre, G., Randles, C., Schulz, M., van Noije, T., Zhang, K., Alados-Arboledas, L., Baltensperger, U., Jefferson, A., Sherman, J., Sun, J., Weingartner, E., and Zieger, P.: A global model-measurement evaluation of particle light scattering coefficients at elevated relative humidity, Atmospheric Chemistry and Physics Discussions, 2020, 1–30, https://doi.org/10.5194/acp-2019-1190, https://www.atmos-chem-phys-discuss.net/acp-2019-1190/, 2020.

Dusek, U., Frank, G. P., Hildebrandt, L., Curtius, J., Schneider, J., Walter, S., Chand, D., Drewnick, F., Hings, S., Jung, D., Borrmann, S., and Andreae, M. O.: Size Matters More Than Chemistry for Cloud-Nucleating Ability of Aerosol Particles, Science, 312, 1375–1378, https://doi.org/10.1126/science.1125261, https://science.sciencemag.org/content/312/5778/1375, 2006.

Janssen, R. H. H., Ganzeveld, L. N., Kabat, P., Kulmala, M., Nieminen, T., and Roebeling, R. A.: Estimating seasonal variations in cloud droplet number concentration over the boreal forest from satellite observations, Atmospheric Chemistry and Physics, 11, 7701–7713, https://doi.org/10.5194/acp-11-7701-2011, https://www.atmos-chem-phys.net/11/7701/2011/, 2011.

Kerminen, V.-M., Chen, X., Vakkari, V., Petäjä, T., Kulmala, M., and Bianchi, F.: Atmospheric new particle formation and growth: review of field observations, Environmental Research Letters, 13, 103 003, https://doi.org/10.1088/1748-9326/aadf3c, https://doi.org/10.1088%2F1748-9326%2Faadf3c, 2018.

Kiehl, J. T. and Briegleb, B. P.: The Relative Roles of Sulfate Aerosols and Greenhouse Gases in Climate Forcing, Science, 260, 311–314, https://doi.org/10.1126/science.260.5106.311, https://science.sciencemag.org/content/260/5106/311, 1993.

Kim, K.-H., Kabir, E., and Kabir, S.: A review on the human health impact of airborne particulate matter, Environment international, 74, 136–143, 2015.

Kipling, Z., Stier, P., Johnson, C. E., Mann, G. W., Bellouin, N., Bauer, S. E., Bergman, T., Chin, M., Diehl, T., Ghan, S. J., Iversen, T., Kirkevåg, A., Kokkola, H., Liu, X., Luo, G., van Noije, T., Pringle, K. J., vonÂ Salzen, K., Schulz, M., Seland, Ø., Skeie, R. B., Takemura, T., Tsigaridis, K., and Zhang, K.: What controls the vertical distribution of aerosol? Relationships between process sensitivity in HadGEM3–UKCA and inter-model variation from AeroCom Phase II, Atmospheric Chemistry and Physics, 16, 2221–2241, https://doi.org/10.5194/acp-16-2221-2016, https://www.atmos-chem-phys.net/16/2221/2016/, 2016.

Koch, D. and Del Genio, A. D.: Black carbon semi-direct effects on cloud cover: review and synthesis, Atmospheric Chemistry and Physics, 10, 7685–7696, https://doi.org/10.5194/acp-10-7685-2010, https://www.atmos-chem-phys.net/10/7685/2010/, 2010.

Krewski, D., Jerrett, M., Burnett, R. T., Ma, R., Hughes, E., Shi, Y., Turner, M. C., Pope III, C. A., Thurston, G., Calle, E. E., et al.: Extended follow-up and spatial analysis of the American Cancer Society study linking particulate air pollution and mortality, 140, Health Effects Institute Boston, MA, 2009.

Kristiansen, N. I., Stohl, A., Olivié, D. J. L., Croft, B., Søvde, O. A., Klein, H., Christoudias, T., Kunkel, D., Leadbetter, S. J., Lee, Y. H., Zhang, K., Tsigaridis, K., Bergman, T., Evangeliou, N., Wang, H., Ma, P.-L., Easter, R. C., Rasch, P. J., Liu, X., Pitari, G., Di Genova, G., Zhao, S. Y., Balkanski, Y., Bauer, S. E., Faluvegi, G. S., Kokkola, H., Martin, R. V., Pierce, J. R., Schulz, M., Shindell, D., Tost, H., and Zhang, H.: Evaluation of observed and modelled aerosol lifetimes using radioactive tracers of opportunity and an ensemble of 19 global models, Atmospheric Chemistry and Physics, 16, 3525–3561, https://doi.org/10.5194/acp-16-3525-2016, https://www.atmos-chem-phys.net/16/3525/2016/, 2016.

Kuwata, M., Kondo, Y., and Takegawa, N.: Critical condensed mass for activation of black carbon as cloud condensation nuclei in Tokyo, Journal of Geophysical Research: Atmospheres, 114, https://doi.org/10.1029/2009JD012086, https://agupubs.onlinelibrary.wiley.com/doi/abs/10.1029/2009JD012086, 2009.

Kühn, T., Partanen, A.-I., Laakso, A., Lu, Z., Bergman, T., Mikkonen, S., Kokkola, H., Korhonen, H., Räisänen, P., Streets, D. G., Romakkaniemi, S., and Laaksonen, A.: Climate impacts of changing aerosol emissions since 1996, Geophysical Research Letters, 41, 4711–4718, https://doi.org/10.1002/2014GL060349, https://agupubs.onlinelibrary.wiley.com/doi/abs/10.1002/2014GL060349, 2014.

Lee, S.-H., Gordon, H., Yu, H., Lehtipalo, K., Haley, R., Li, Y., and Zhang, R.: New Particle Formation in the Atmosphere: From Molecular Clusters to Global Climate, Journal of Geophysical Research: Atmospheres, 124, 7098–7146, https://doi.org/10.1029/2018JD029356, https://agupubs.onlinelibrary.wiley.com/doi/abs/10.1029/2018JD029356, 2019.

Menon, S., Koch, D., Beig, G., Sahu, S., Fasullo, J., and Orlikowski, D.: Black carbon aerosols and the third polar ice cap, Atmospheric Chemistry and Physics, 10, 4559–4571, https://doi.org/10.5194/acp-10-4559-2010, https://www.atmos-chem-phys.net/10/4559/2010/, 2010.

Partanen, A.-I., Landry, J.-S., and Matthews, H. D.: Climate and health implications of future aerosol emission scenarios, Environmental Research Letters, 13, 024 028, https://doi.org/10.1088/1748-9326/aaa511, https://iopscience.iop.org/article/10.1088/1748-9326/aaa511/meta, 2018.

Pope III, C. A., Burnett, R. T., Thun, M. J., Calle, E. E., Krewski, D., Ito, K., and Thurston, G. D.: Lung Cancer, Cardiopulmonary Mortality, and Long-term Exposure to Fine Particulate Air Pollution, JAMA, 287, 1132–1141, https://doi.org/10.1001/jama.287.9.1132, https://doi.org/10.1001/jama.287.9.1132, 2002.

Ramanathan, V. and Carmichael, G.: Global and regional climate changes due to black carbon, Nature geoscience, 1, 221–227, 2008.

Samset, B. H. and Myhre, G.: Vertical dependence of black carbon, sulphate and biomass burning aerosol radiative forcing, Geophysical Research Letters, 38, https://doi.org/10.1029/2011GL049697, https://agupubs.onlinelibrary.wiley.com/doi/abs/10.1029/2011GL049697, 2011.

Saponaro, G., Sporre, M. K., Neubauer, D., Kokkola, H., Kolmonen, P., Sogacheva, L., Arola, A., de Leeuw, G., Karset, I. H. H., Laaksonen, A., and Lohmann, U.: Evaluation of aerosol and cloud properties in three climate models using MODIS observations and its corresponding COSP simulator, as well as their application in aerosol–cloud interactions, Atmospheric Chemistry and Physics, 20, 1607–1626, https://doi.org/10.5194/acp-20-1607-2020, https://www.atmos-chem-phys.net/20/1607/2020/, 2020.

Tröstl, J., Chuang, W. K., Gordon, H., Heinritzi, M., Yan, C., Molteni, U., Ahlm, L., Frege, C., Bianchi, F., Wagner, R., et al.: The role of low-volatility organic compounds in initial particle growth in the atmosphere, Nature, 533, 527–531, 2016.

Tsigaridis, K., Daskalakis, N., Kanakidou, M., Adams, P. J., Artaxo, P., Bahadur, R., Balkanski, Y., Bauer, S. E., Bellouin, N., Benedetti, A., Bergman, T., Berntsen, T. K., Beukes, J. P., Bian, H., Carslaw, K. S., Chin, M., Curci, G., Diehl, T., Easter, R. C., Ghan, S. J., Gong, S. L., Hodzic, A., Hoyle, C. R., Iversen, T., Jathar, S., Jimenez, J. L., Kaiser, J. W., Kirkevåg, A., Koch, D., Kokkola, H., Lee, Y. H., Lin, G., Liu, X., Luo, G., Ma, X., Mann, G. W., Mihalopoulos, N., Morcrette, J.-J., Müller, J.-F., Myhre, G., Myriokefalitakis, S., Ng, N. L., O'Donnell, D., Penner, J. E., Pozzoli, L., Pringle, K. J., Russell, L. M., Schulz, M., Sciare, J., Seland, Ø., Shindell, D. T., Sillman, S., Skeie, R. B., Spracklen, D., Stavrakou, T., Steenrod, S. D., Takemura, T., Tiitta, P., Tilmes, S., Tost, H., van Noije, T., van Zyl, P. G., von Salzen, K., Yu, F., Wang, Z., Wang, Z., Zaveri, R. A., Zhang, H., Zhang, K., Zhang, Q., and Zhang, X.: The AeroCom evaluation and intercomparison of organic aerosol in global models, Atmospheric Chemistry and Physics, 14, 10 845–10 895, https://doi.org/10.5194/acp-14-10845-2014, https://www.atmos-chem-phys.net/14/10845/2014/, 2014.

United Nations, E. B. f. t. C. o. L.-r. T. A. P.: Protocol to Abate Acidification, Eutrophication and Ground-level Ozone to the Convention on Longrange Transboundary Air Pollution, http://www.unece.org/env/lrtap/multi_h1.html, 1999.

Winiger, P., Barrett, T. E., Sheesley, R. J., Huang, L., Sharma, S., Barrie, L. A., Yttri, K. E., Evangeliou, N., Eckhardt, S., Stohl, A., Klimont, Z., Heyes, C., Semiletov, I. P., Dudarev, O. V., Charkin, A., Shakhova, N., Holmstrand, H., Andersson, A., and Gustafsson, Ö.: Source apportionment of circum-Arctic atmospheric black carbon from isotopes and modeling, Science Advances, 5, https://doi.org/10.1126/sciadv.aau8052, https://advances.sciencemag.org/content/5/2/eaau8052, 2019.

Diehl, T., Heil, A., Chin, M., Pan, X., Streets, D., Schultz, M., and Kinne, S.: Anthropogenic, biomass burning, and volcanic emissions of black carbon, organic carbon, and SO_2 from 1980 to 2010 for hindcast model experiments, Atmospheric Chemistry and Physics Discussions, 12, 24 895–24 954, https://doi.org/10.5194/acpd-12-24895-2012, https://www.atmos-chem-phys-discuss.net/12/24895/2012/, 2012.

Doherty, S. J., Bitz, C. M., and Flanner, M. G.: Biases in modeled surface snow BC mixing ratios in prescribed-aerosol climate model runs, Atmospheric Chemistry and Physics, 14, 11 697–11 709, https://doi.org/10.5194/acp-14-11697-2014, https://www.atmos-chem-phys.net/14/11697/2014/, 2014.

Forster, P. M., Richardson, T., Maycock, A. C., Smith, C. J., Samset, B. H., Myhre, G., Andrews, T., Pincus, R., and Schulz, M.: Recommendations for diagnosing effective radiative forcing from climate models for CMIP6, Journal of Geophysical Research: Atmospheres, 121, 12,460–12,475, https://doi.org/10.1002/2016JD025320, https://agupubs.onlinelibrary.wiley.com/doi/abs/10.1002/2016JD025320, 2016.

Goldberg, E. D.: Black carbon in the environment: properties and distribution, J. Wiley New York, 1985.

Granier, C., Bessagnet, B., Bond, T., D'Angiola, A., Denier van der Gon, H., Frost, G. J., Heil, A., Kaiser, J. W., Kinne, S., Klimont, Z., Kloster, S., Lamarque, J.-F., Liousse, C., Masui, T., Meleux, F., Mieville, A., Ohara, T., Raut, J.-C., Riahi, K., Schultz, M. G., Smith, S. J., Thompson, A., van Aardenne, J., van der Werf, G. R., and van Vuuren, D. P.: Evolution of anthropogenic and biomass burning emissions of air pollutants at global and regional scales during the 1980–2010 period, Climatic Change, 109, 163, https://doi.org/10.1007/s10584-011-0154-1, https://doi.org/10.1007/s10584-011-0154-1, 2011.

Huijnen, V., Williams, J., van Weele, M., van Noije, T., Krol, M., Dentener, F., Segers, A., Houweling, S., Peters, W., de Laat, J., Boersma, F., Bergamaschi, P., van Velthoven, P., Le Sager, P., Eskes, H., Alkemade, F., Scheele, R., Nédélec, P., and Pätz, H.-W.: The global chemistry transport model TM5: description and evaluation of the tropospheric chemistry version 3.0, Geoscientific Model Development, 3, 445–473, https://doi.org/10.5194/gmd-3-445-2010, https://www.geosci-model-dev.net/3/445/2010/, 2010.

Inness, A., Baier, F., Benedetti, A., Bouarar, I., Chabrillat, S., Clark, H., Clerbaux, C., Coheur, P., Engelen, R. J., Errera, Q., Flemming, J., George, M., Granier, C., Hadji-Lazaro, J., Huijnen, V., Hurtmans, D., Jones, L., Kaiser, J. W., Kapsomenakis, J., Lefever, K., Leitão, J., Razinger, M., Richter, A., Schultz, M. G., Simmons, A. J., Suttie, M., Stein, O., Thépaut, J.-N., Thouret, V., Vrekoussis, M., Zerefos, C., and the MACC team: The MACC reanalysis: an 8 yr data set of atmospheric composition, Atmospheric Chemistry and Physics, 13, 4073–4109, https://doi.org/10.5194/acp-13-4073-2013, https://www.atmos-chem-phys.net/13/4073/2013/, 2013.

IPCC: Annex II: Climate System Scenario Tables, book section AII, p. 1395–1446, Cambridge University Press, Cambridge, United Kingdom and New York, NY, USA, https://doi.org/10.1017/CBO9781107415324.030, www.climatechange2013.org, 2013.

Jiao, C., Flanner, M. G., Balkanski, Y., Bauer, S. E., Bellouin, N., Berntsen, T. K., Bian, H., Carslaw, K. S., Chin, M., De Luca, N., Diehl, T., Ghan, S. J., Iversen, T., Kirkevåg, A., Koch, D., Liu, X., Mann, G. W., Penner, J. E., Pitari, G., Schulz, M., Seland, Ø., Skeie, R. B., Steenrod, S. D., Stier, P., Takemura, T., Tsigaridis, K., van Noije, T., Yun, Y., and Zhang, K.: An AeroCom assessment of black carbon in Arctic snow and sea ice, Atmospheric Chemistry and Physics, 14, 2399–2417, https://doi.org/10.5194/acp-14-2399-2014, https://www.atmos-chem-phys.net/14/2399/2014/, 2014.

Klimont, Z., Kupiainen, K., Heyes, C., Purohit, P., Cofala, J., Rafaj, P., Borken-Kleefeld, J., and Schöpp, W.: Global anthropogenic emissions of particulate matter including black carbon, Atmospheric Chemistry and Physics, 17, 8681–8723, https://doi.org/10.5194/acp-17-8681-2017, https://www.atmos-chem-phys.net/17/8681/2017/, 2017.

Kokkola, H., Kühn, T., Laakso, A., Bergman, T., Lehtinen, K. E. J., Mielonen, T., Arola, A., Stadtler, S., Korhonen, H., Ferrachat, S., Lohmann, U., Neubauer, D., Tegen, I., Siegenthaler-Le Drian, C., Schultz, M. G., Bey, I., Stier, P., Daskalakis, N., Heald, C. L., and Romakkaniemi, S.: SALSA2.0: The sectional aerosol module of the aerosol–chemistry–climate model ECHAM6.3.0-HAM2.3-MOZ1.0, Geoscientific Model Development, 11, 3833–3863, https://doi.org/10.5194/gmd-11-3833-2018, https://www.geosci-model-dev.net/11/3833/2018/, 2018.

Lim, S. S., Vos, T., Flaxman, A. D., Danaei, G., Shibuya, K., Adair-Rohani, H., AlMazroa, M. A., Amann, M., Anderson, H. R., Andrews, K. G., Aryee, M., Atkinson, C., Bacchus, L. J., Bahalim, A. N., Balakrishnan, K., Balmes, J., Barker-Collo, S., Baxter, A., Bell, M. L., Blore, J. D., Blyth, F., Bonner, C., Borges, G., Bourne, R., Boussinesq, M., Brauer, M., Brooks, P., Bruce, N. G., Brunekreef, B., Bryan-Hancock, C., Bucello, C., Buchbinder, R., Bull, F., Burnett, R. T., Byers, T. E., Calabria, B., Carapetis, J., Carnahan, E., Chafe, Z., Charlson, F., Chen, H., Chen, J. S., Cheng, A. T.-A., Child, J. C., Cohen, A., Colson, K. E., Cowie, B. C., Darby, S., Darling, S., Davis, A.,

Degenhardt, L., Dentener, F., Jarlais, D. C. D., Devries, K., Dherani, M., Ding, E. L., Dorsey, E. R., Driscoll, T., Edmond, K., Ali, S. E., Engell, R. E., Erwin, P. J., Fahimi, S., Falder, G., Farzadfar, F., Ferrari, A., Finucane, M. M., Flaxman, S., Fowkes, F. G. R., Freedman, G., Freeman, M. K., Gakidou, E., Ghosh, S., Giovannucci, E., Gmel, G., Graham, K., Grainger, R., Grant, B., Gunnell, D., Gutierrez, H. R., Hall, W., Hoek, H. W., Hogan, A., Hosgood, H. D., Hoy, D., Hu, H., Hubbell, B. J., Hutchings, S. J., Ibeanusi, S. E., Jacklyn, G. L., Jasrasaria, R., Jonas, J. B., Kan, H., Kanis, J. A., Kassebaum, N., Kawakami, N., Khang, Y.-H., Khatibzadeh, S., Khoo, J.-P., Kok, C., Laden, F., Lalloo, R., Lan, Q., Lathlean, T., Leasher, J. L., Leigh, J., Li, Y., Lin, J. K., Lipshultz, S. E., London, S., Lozano, R., Lu, Y., Mak, J., Malekzadeh, R., Mallinger, L., Marcenes, W., March, L., Marks, R., Martin, R., McGale, P., McGrath, J., Mehta, S., Memish, Z. A., Mensah, G. A., Merriman, T. R., Micha, R., Michaud, C., Mishra, V., Hanafiah, K. M., Mokdad, A. A., Morawska, L., Mozaffarian, D., Murphy, T., Naghavi, M., Neal, B., Nelson, P. K., Nolla, J. M., Norman, R. E., Olives, C., Omer, S. B., Orchard, J., Osborne, R., Ostro, B., Page, A., Pandey, K. D., Parry, C. D., Passmore, E., Patra, J., Pearce, N., Pelizzari, P. M., Petzold, M., Phillips, M. R., Pope, D., Pope, C. A., Powles, J., Rao, M., Razavi, H., Rehfuess, E. A., Rehm, J. T., Ritz, B., Rivara, F. P., Roberts, T., Robinson, C., Rodriguez-Portales, J. A., Romieu, I., Room, R., Rosenfeld, L. C., Roy, A., Rushton, L., Salomon, J. A., Sampson, U., Sanchez-Riera, L., Sanman, E., Sapkota, A., Seedat, S., Shi, P., Shield, K., Shivakoti, R., Singh, G. M., Sleet, D. A., Smith, E., Smith, K. R., Stapelberg, N. J., Steenland, K., Stöckl, H., Stovner, L. J., Straif, K., Straney, L., Thurston, G. D., Tran, J. H., Dingenen, R. V., van Donkelaar, A., Veerman, J. L., Vijayakumar, L., Weintraub, R., Weissman, M. M., White, R. A., Whiteford, H., Wiersma, S. T., Wilkinson, J. D., Williams, H. C., Williams, W., Wilson, N., Woolf, A. D., Yip, P., Zielinski, J. M., Lopez, A. D., Murray, C. J., and Ezzati, M.: A comparative risk assessment of burden of disease and injury attributable to 67 risk factors and risk factor clusters in 21 regions, 1990–2010: A systematic analysis for the Global Burden of Disease Study 2010, The Lancet, 380, 2224–2260, https://doi.org/10.1016/S0140-6736(12)61766-8, https://eprints.qut.edu.au/84325/, 2012.

Lohmann, U., Rotstayn, L., Storelvmo, T., Jones, A., Menon, S., Quaas, J., Ekman, A. M. L., Koch, D., and Ruedy, R.: Total aerosol effect: radiative forcing or radiative flux perturbation?, Atmospheric Chemistry and Physics, 10, 3235–3246, https://doi.org/10.5194/acp-10-3235-2010, https://www.atmos-chem-phys.net/10/3235/2010/, 2010.

Quinn, P. K., Stohl, A., Arneth, A., Berntsen, T., Burkhart, J. F., Christensen, J., Flanner, M., Kupiainen, K., Lihavainen, H., Shepherd, M., V., S., H., S., and V., V.: The impact of black carbon on Arctic climate, Arctic Monitoring and Assessment Programme (AMAP), 2011.

Ramanathan, V., Cess, R. D., Harrison, E. F., Minnis, P., Barkstrom, B. R., Ahmad, E., and Hartmann, D.: Cloud-Radiative Forcing and Climate: Results from the Earth Radiation Budget Experiment, Science, 243, 57–63, https://doi.org/10.1126/science.243.4887.57, https://science.sciencemag.org/content/243/4887/57, 1989.

Samset, B. H. and Myhre, G.: Climate response to externally mixed black carbon as a function of altitude, Journal of Geophysical Research: Atmospheres, 120, 2913–2927, https://doi.org/10.1002/2014JD022849, https://agupubs.onlinelibrary.wiley.com/doi/abs/10.1002/2014JD022849, 2015.

Sand, M., Berntsen, T. K., Von Salzen, K., Flanner, M. G., Langner, J., and Victor, D. G.: Response of Arctic temperature to changes in emissions of short-lived climate forcers, Nature Climate Change, 6, 286, 2016.

Schultz, M. G., Stadtler, S., Schröder, S., Taraborrelli, D., Franco, B., Krefting, J., Henrot, A., Ferrachat, S., Lohmann, U., Neubauer, D., Siegenthaler-Le Drian, C., Wahl, S., Kokkola, H., Kühn, T., Rast, S., Schmidt, H., Stier, P., Kinnison, D., Tyndall, G. S., Orlando, J. J., and Wespes, C.: The chemistry–climate model ECHAM6.3-HAM2.3-MOZ1.0, Geoscientific Model Development, 11, 1695–1723, https://doi.org/10.5194/gmd-11-1695-2018, https://www.geosci-model-dev.net/11/1695/2018/, 2018.

Shindell, D., Kuylenstierna, J. C. I., Vignati, E., van Dingenen, R., Amann, M., Klimont, Z., Anenberg, S. C., Muller, N., Janssens-Maenhout, G., Raes, F., Schwartz, J., Faluvegi, G., Pozzoli, L., Kupiainen, K., Höglund-Isaksson, L., Emberson, L., Streets, D., Ra-

manathan, V., Hicks, K., Oanh, N. T. K., Milly, G., Williams, M., Demkine, V., and Fowler, D.: Simultaneously Mitigating Near-Term Climate Change and Improving Human Health and Food Security, Science, 335, 183–189, https://doi.org/10.1126/science.1210026, https://science.sciencemag.org/content/335/6065/183, 2012.

Smith, C. J., Kramer, R. J., Myhre, G., Forster, P. M., Soden, B. J., Andrews, T., Boucher, O., Faluvegi, G., Fläschner, D., Hodnebrog, Ø., Kasoar, M., Kharin, V., Kirkevåg, A., Lamarque, J.-F., Mülmenstädt, J., Olivié, D., Richardson, T., Samset, B. H., Shindell, D., Stier, P., Takemura, T., Voulgarakis, A., and Watson-Parris, D.: Understanding Rapid Adjustments to Diverse Forcing Agents, Geophysical Research Letters, 45, 12,023–12,031, https://doi.org/10.1029/2018GL079826, https://agupubs.onlinelibrary.wiley.com/doi/abs/10.1029/2018GL079826, 2018.

Stevens, B., Giorgetta, M., Esch, M., Mauritsen, T., Crueger, T., Rast, S., Salzmann, M., Schmidt, H., Bader, J., Block, K., Brokopf, R., Fast, I., Kinne, S., Kornblueh, L., Lohmann, U., Pincus, R., Reichler, T., and Roeckner, E.: Atmospheric component of the MPI-M Earth System Model: ECHAM6, Journal of Advances in Modeling Earth Systems, 5, 146–172, https://doi.org/10.1002/jame.20015, https://agupubs.onlinelibrary.wiley.com/doi/abs/10.1002/jame.20015, 2013.

Stocker, T., Qin, D., Plattner, G.-K., Alexander, L., Allen, S., Bindoff, N., Bréon, F.-M., Church, J., Cubasch, U., Emori, S., Forster, P., Friedlingstein, P., Gillett, N., Gregory, J., Hartmann, D., Jansen, E., Kirtman, B., Knutti, R., Krishna Kumar, K., Lemke, P., Marotzke, J., Masson-Delmotte, V., Meehl, G., Mokhov, I., Piao, S., Ramaswamy, V., Randall, D., Rhein, M., Rojas, M., Sabine, C., Shindell, D., Talley, L., Vaughan, D., and Xie, S.-P.: Technical Summary, book section TS, p. 33–115, Cambridge University Press, Cambridge, United Kingdom and New York, NY, USA, https://doi.org/10.1017/CBO9781107415324.005, www.climatechange2013.org, 2013.

Stohl, A.: Characteristics of atmospheric transport into the Arctic troposphere, Journal of Geophysical Research: Atmospheres, 111, https://doi.org/10.1029/2005JD006888, https://agupubs.onlinelibrary.wiley.com/doi/abs/10.1029/2005JD006888, 2006.

Stohl, A., Klimont, Z., Eckhardt, S., Kupiainen, K., Shevchenko, V. P., Kopeikin, V. M., and Novigatsky, A. N.: Black carbon in the Arctic: the underestimated role of gas flaring and residential combustion emissions, Atmospheric Chemistry and Physics, 13, 8833–8855, https://doi.org/10.5194/acp-13-8833-2013, https://www.atmos-chem-phys.net/13/8833/2013/, 2013.

Stohl, A., Aamaas, B., Amann, M., Baker, L. H., Bellouin, N., Berntsen, T. K., Boucher, O., Cherian, R., Collins, W., Daskalakis, N., Dusinska, M., Eckhardt, S., Fuglestvedt, J. S., Harju, M., Heyes, C., Hodnebrog, Ø., Hao, J., Im, U., Kanakidou, M., Klimont, Z., Kupiainen, K., Law, K. S., Lund, M. T., Maas, R., MacIntosh, C. R., Myhre, G., Myriokefalitakis, S., Olivié, D., Quaas, J., Quennehen, B., Raut, J.-C., Rumbold, S. T., Samset, B. H., Schulz, M., Seland, Ø., Shine, K. P., Skeie, R. B., Wang, S., Yttri, K. E., and Zhu, T.: Evaluating the climate and air quality impacts of short-lived pollutants, Atmospheric Chemistry and Physics, 15, 10 529–10 566, https://doi.org/10.5194/acp-15-10529-2015, https://www.atmos-chem-phys.net/15/10529/2015/, 2015.

Storelvmo, T., Lohmann, U., and Bennartz, R.: What governs the spread in shortwave forcings in the transient IPCC AR4 models?, Geophysical Research Letters, 36, https://doi.org/10.1029/2008GL036069, https://agupubs.onlinelibrary.wiley.com/doi/abs/10.1029/2008GL036069, 2009.

Taylor, K. E., Stouffer, R. J., and Meehl, G. A.: An Overview of CMIP5 and the Experiment Design, Bulletin of the American Meteorological Society, 93, 485–498, https://doi.org/10.1175/BAMS-D-11-00094.1, https://doi.org/10.1175/BAMS-D-11-00094.1, 2012.

Tegen, I., Neubauer, D., Ferrachat, S., Siegenthaler-Le Drian, C., Bey, I., Schutgens, N., Stier, P., Watson-Parris, D., Stanelle, T., Schmidt, H., Rast, S., Kokkola, H., Schultz, M., Schroeder, S., Daskalakis, N., Barthel, S., Heinold, B., and Lohmann, U.: The aerosol-climate model ECHAM6.3-HAM2.3: Aerosol evaluation, Geoscientific Model Development Discussions, 2018, 1–54, https://doi.org/10.5194/gmd-2018-235, https://www.geosci-model-dev-discuss.net/gmd-2018-235/, 2018.

Twomey, S.: The Influence of Pollution on the Shortwave Albedo of Clouds, Journal of the Atmospheric Sciences, 34, 1149–1152, https://doi.org/10.1175/1520-0469(1977)034<1149:TIOPOT>2.0.CO;2, https://doi.org/10.1175/1520-0469(1977)034<1149:TIOPOT>2.0.CO;2, 1977.

Van Dingenen, R., Dentener, F., Crippa, M., Leitao, J., Marmer, E., Rao, S., Solazzo, E., and Valentini, L.: TM5-FASST: a global atmospheric source–receptor model for rapid impact analysis of emission changes on air quality and short-lived climate pollutants, Atmospheric Chemistry and Physics, 18, 16 173–16 211, https://doi.org/10.5194/acp-18-16173-2018, https://www.atmos-chem-phys.net/18/16173/2018/, 2018.

Yang, Q., Bitz, C. M., and Doherty, S. J.: Offsetting effects of aerosols on Arctic and global climate in the late 20th century, Atmospheric Chemistry and Physics, 14, 3969–3975, https://doi.org/10.5194/acp-14-3969-2014, https://www.atmos-chem-phys.net/14/3969/2014/, 2014.

Zhang, K., Wan, H., Liu, X., Ghan, S. J., Kooperman, G. J., Ma, P.-L., Rasch, P. J., Neubauer, D., and Lohmann, U.: Technical Note: On the use of nudging for aerosol-climate model intercomparison studies, Atmospheric Chemistry and Physics, 14, 8631–8645, https://doi.org/10.5194/acp-14-8631-2014, https://www.atmos-chem-phys.net/14/8631/2014/, 2014.